Early life stress-induced miR-708-5p affects bipolar disorder-associated phenotypes through neuronatin downregulation.

Carlotta Gilardi[1], Helena C. Martins[1], Alessandra Lo Bianco[1], Silvia Bicker[1], Pierre-Luc Germain[1,2,3], Fridolin Gross[1*], Ayse Özge Sungur[4,5,6,7], Theresa M. Kisko[4,5,6,7], Frederike Stein[8], Susanne Meinert[9], Rainer K. W. Schwarting[4], Markus Wöhr[4,5,6,7], Udo Dannlowski[9], Tilo Kircher[8], and Gerhard Schratt[1§]

1 ETH Zurich, Lab of Systems Neuroscience, Institute for Neuroscience, Department of Health Science and Technology, 8057 Zurich, Switzerland

2 Laboratory of Molecular and Behavioural Neuroscience, Institute for Neuroscience, Department of Health Science and Technology, ETH Zürich, Switzerland

3 Lab of Statistical Bioinformatics, IMLS, University of Zürich, Switzerland

4 Philipps-University of Marburg, Faculty of Psychology, Experimental and Biological Psychology, Behavioral Neuroscience, D-35032 Marburg, Germany

5 Center for Mind, Brain and Behavior, D-35032 Marburg, Germany

6 KU Leuven, Faculty of Psychology and Educational Sciences, Research Unit Brain and Cognition, Laboratory of Biological Psychology, Social and Affective Neuroscience Research Group, B-3000 Leuven, Belgium.

7 KU Leuven, Leuven Brain Institute, B-3000 Leuven, Belgium

8 Department of Psychiatry and Psychotherapy, University of Marburg, Marburg, Germany.

9 Institute for Translational Psychiatry, University of Münster, Münster, Germany.

*current address: CNRS UMR5164 ImmunoConcEpT, University of Bordeaux, France

§: to whom correspondence should be addressed: Gerhard.schratt@hest.ethz.ch

Running title: miR-708-5p in bipolar disorder

Abstract

The underlying physiological and molecular mechanisms of bipolar disorder (BD) remain largely unknown. Here, by using unbiased small RNA sequencing in peripheral blood mononuclear cells (PBMCs), we found that miR-708-5p, a microRNA that was previously associated with BD, is the most strongly upregulated microRNA in peripheral blood of both healthy human subjects with a high genetic or environmental predisposition to develop mood disorders (MDs). Furthermore, miR-708-5p is strongly upregulated in patients diagnosed with BD and has potential in conjunction with the previously identified miR-499-5p to differentiate BD patients from patients suffering from major depressive disorder (MDD) and healthy controls. miR-708 is also upregulated in the hippocampus of wild type juvenile rats that underwent social isolation, as well as in juvenile rats heterozygous for the BD risk gene *Cacna1c*. Furthermore, ectopic overexpression of miR-708-5p in the hippocampus of adult male mice leads to BD-associated endophenotypes, such as reduced behavioral despair, enhanced compulsivity, and short-term memory impairments. miR-708-5p directly targets Neuronatin (Nnat), an endoplasmic reticulum (ER) resident protein involved in calcium homeostasis. Restoring Nnat expression in the hippocampus of miR-708-5p overexpressing mice rescues BD-associated endophenotypes. In summary, we functionally link miR-708-5p dependent regulation of Nnat to BD, with potential implications for BD diagnosis and therapy.

53 # Introduction

54 MDs are a group of chronic psychiatric diseases affecting mood and cognition that
55 include Major Depressive Disorder (MDD) and Bipolar Disorder (BD). MDD is
56 characterized by long, persistent, depressive episodes. BD has a distinct pattern of
57 mood oscillations, from depressive episodes like MDD, and (hypo)manic phases.
58 Furthermore, BD is subclassified in BD type 1 (mania and depression), and BD type 2
59 (hypomania and depression). It is known that MDs are highly heritable and share
60 common genetic signature (1). In particular, BD is characterized by up to 70%
61 heritability in monozygotic twins (2). However, complex polygenetic mechanisms
62 cannot fully explain the onset of BD, and environmental factors, such as early life
63 stress, play an important role in the etiology and outcome of BD (3–5). Furthermore,
64 BD presents sex-specific mood and cognitive features. Manic episode onset occurs
65 earlier in life in men (6,7), while women experience more depressive episodes (6).
66 From the cognitive side, men perform worse in recognition memory tasks than
67 women, but they do better in working memory tests (8).

68 Preclinical studies have employed genetic and environmental animal models of BD,
69 most of them mimicking the manic or the depressive phase of the disease. Several
70 environmental and genetic mouse models, e.g., sleep deprivation (9), deficiency of
71 the circadian regulator *Clock* (10) or the cytoskeleton regulator *Ank3* (ANK-G) (11),
72 recapitulate aspects of the manic endophenotypes of BD. They display reduced
73 immobility in the forced swim test (FST), an effect which models reduced helplessness
74 and antidepressant-like behavior. Furthermore, they show reduced anxiety in the
75 open field test (OFT), and higher preference for reward stimuli and hedonic behavior
76 (sucrose, cocaine) (10). Similarly, when the lithium target GSK3β is pharmacologically
77 inhibited, mice show no mania-like behavior in the amphetamine-induced
78 hyperactivity test (12). Mice haplo-insufficient for the cross-psychiatric risk gene
79 *Cacna1c* show decreased immobility in the tail suspension test (TST) and FST, higher
80 preference for sucrose as well as decreased anxiety behavior, although the latter was
81 a characteristic of female mice only (13).

82 Recent research has highlighted the role of microRNAs (miRNAs) in the pathogenesis
83 and their potential for treatment of MDs, including BD (14). miRNAs are a large family

84 of small (~22nt), noncoding RNAs that act as posttranscriptional regulators by
85 binding to complementary sequences in the 3′- untranslated region (UTR) of target
86 messenger RNAs (mRNAs) (15). miRNAs are widely expressed in the brain, where they
87 regulate neuroplasticity (16) and cellular stress responses (17). They have been
88 associated with BD etiology in expression studies of postmortem brain tissue of BD
89 patients (18). Furthermore, lithium and valproic acid (VPA), the primary mood
90 stabilizers used in BD treatment, affect miRNA expression (19,20). Variants in miRNA
91 genes associated with a higher risk of BD have been identified (21), and manipulation
92 of one of these miRNAs (miR-499-5p) caused cognitive impairments and mood
93 disorder-related endophenotypes in rats (14,22). However, most miRNAs
94 dysregulated in BD have not been functionally investigated, and the molecular
95 mechanisms by which they control BD-associated endophenotypes remain largely
96 unknown. Differential expression of miRNAs in peripheral blood mononuclear cells
97 (PBMCs) has been often investigated for biomarker discovery in psychiatric disorders.
98 For example, miR-499-5p was significantly upregulated in female and male PBMC
99 samples of BD (22). miR-124-3p was found to be significantly upregulated in PBMCs
100 samples of MDD compared to healthy controls and it was downregulated after eight
101 weeks of antidepressant treatment (23). miR-30a-5p was downregulated in the
102 PBMCs of unmedicated patients in acute state schizophrenia (SCZ) and upregulated
103 following antipsychotic treatment (24). However, these attempts so far have not
104 yielded reliable miRNA biomarkers in MDs, especially regarding the differential
105 diagnosis of BD and MDD.

106 In this study, we identified miRNA-708-5p as a miRNA whose expression is induced
107 by genetic and environmental risk in rats and humans. Previous studies already
108 pointed to a potential role of miR-708-5p in the development of MDs. miR-708-5p is
109 nominally associated with BD in GWAS (21) and it originates from the first intron of
110 *ODZ4*, a protein-coding gene which is also significantly associated with BD (25).
111 Moreover, both *ODZ4* and miR-708-5p expression are stress susceptible (26–28). It
112 was shown that the synthetic glucocorticoid dexamethasone (DEX) upregulates
113 *ODZ4* and miR-708-5p in the context of ovarian cancer (29). Moreover,
114 CCAAT/enhancer binding protein (C/EBP) homologous protein (CHOP) can induce
115 *ODZ4* and miR-708-5p expression upon ER stress activation (30). A recent study

116 reported miR-708-5p upregulation in the PFC upon seven days of chronic social
117 defeat in vulnerable rats compared to resilient animals (31).

118 Neuronatin (Nnat) was previously identified as a target of miR-708-5p (26,28,32–34).
119 It is a small protein bound to the Endoplasmic Reticulum (ER) membrane that
120 antagonizes the activity of sarco-endoplasmic reticulum calcium ATPase (SERCA),
121 thereby regulating calcium re-uptake from the cytosol to the ER (35,36). In neurons,
122 Nnat controls dendritic calcium transients (32) and intracellular calcium levels in the
123 context of Angelman syndrome (33). Intriguingly, both ER stress (37) and
124 dysregulated calcium homeostasis (38) have been repeatedly linked to BD. The
125 importance of the miR-708-5p/Nnat pathway for MDs, however, has not yet been
126 investigated.

127

Materials and Methods

Human study

Recruitment of Participants

The study involved participants with BD (26 females, 37 males), MDD (18 females, 24 males), and healthy individuals (26 females, 31 males), including psychiatrically healthy subjects that had a history of childhood maltreatment (17) or a genetic predisposition to MDs (18) or no risk (18). MDsThese participants were recruited from the University of Marburg and the University of Münster in Germany, as part of the FOR2107 cohort (39). Diagnoses were made using the SCID-I interview (40), and adapted to DSM-IV criteria (41), excluding those with substance abuse, severe neurological, or other significant medical conditions. Healthy controls were screened similarly, with inclusion in the maltreatment study if at least one of the subclasses of the Childhood Trauma Questionnaire (CTQ) reached the maltreatment threshold (Emotional Abuse ≥ 10, Physical Abuse ≥ 8, Sexual Abuse ≥ 8, Emotional Neglect ≥ 15, and Physical Neglect ≥ 8) (42). All participants underwent a comprehensive neuropsychological test battery, including the d2 test of attention (43). All necessary ethical approvals were obtained (ethics committees of the Medical Faculties of the Universities of Münster (2014-422-b-S) and Marburg (AZ: 07/14)), and participants consented to the study, which complied with the Declaration of Helsinki and the Belmont Report. Demographic and clinical data are outlined in Table 1 and in Supplementary Table 1.

Human peripheral blood mononuclear cell (PBMC) sample processing.

PBMCs were obtained from 10 ml of whole blood using the LeukoLOCK technology (Thermo Scientific) at the Biomaterialbank Marburg, Germany. After sample randomization, total RNA extraction from PBMCs was carried out using the *mir*Vana™ kit (Thermo Fisher) or TRIzol™ Reagent (Thermo Fisher) following the manufacturer's protocol.

156 ## PBMCs processing for small RNA-sequencing

157 For the Small RNA-sequencing, RNA was extracted with *mir*Vana™ kit (Thermo
158 Fisher) and DNase treated, and it was carried out at Functional Genomic Center
159 Zurich (FGCZ, https://fgcz.ch/).

160 ## Small RNA-analysis

161 Short RNA reads were processed using the ncPro 1.6.4 pipeline (44) using the hg19
162 annotated (based on miRBase version 21). Only mature miRNA reads (accepting
163 +2bp on either end) were considered for downstream analysis. Differential
164 expression analysis was then performed using limma/voom 3.46.0 (45), with a model
165 including a covariate to correct for the two technical batches.

166 ## *Rat primary neuron culture*

167 Cultures of primary hippocampal and cortical neurons from rat hippocampus were
168 established using E18 Sprague-Dawley rats obtained from Janvier Laboratories, as
169 described previously (22).

170 ## Transfection

171 Primary hippocampal neurons were transfected with Lipofectamine™ 2000 Reagent
172 and plasmid DNA constructs as previously described (22).

173 ## Virus infection

174 Primary hippocampal neurons were infected with recombinant adeno-associated
175 virus (rAAV) containing hpCTL or hp708 constructs on *days in vitro* (DIV) 2 by adding
176 300µl of a mixture of the virus with 300µl of NBP+ per well of a 24-well plate. Cells
177 were used for downstream analysis on DIV19-20.

178 ## Luciferase Assay

179 DIV6 hippocampal neurons were transfected with 100ng of the Nnat-3'UTR
180 luciferase reporters and 500ng of hpCTL-p or hp708-p, spCTL-p or sp708-p. After
181 seven days from transfection, the cells were lysed, luciferase assay was conducted
182 using a GloMax R96 Microplate Luminometer (Promega), as previously described
183 (22). The relative luciferase activity was determined by calculating the ratio of the
184 Firefly signal to the Renilla signal.

185 ## *In Situ* Hybridization

186 Single-molecule fluorescence *in situ* hybridization (smFISH) for miRNA detection in
187 hippocampal neuron cultures was conducted using the QuantiGene ViewRNA
188 miRNA Cell Assay Kit (Thermo Fisher, QVCM0001) following the manufacturer
189 protocol with minor adjustments. Probes for has-miR-708-5p (Alexa Fluor 546,
190 Thermo Fisher), Nnat (Alexa Fluor 546), CamK2 (Alexa Fluor 488) and Gad2 (Alexa
191 Fluor 488) were used for the assay.

192 ## *Plasmid design and rAAVs preparation*

193 For rAAV-mediated overexpression of miR-708-5p, the chimeric miR-708 hairpin was
194 generated by polynucleotide cloning. A detailed description and characterization of
195 this system have been published (14,46). To knockdown miR-708-5p, a sponge
196 plasmid was constructed by inserting six TDMD sites predicted to bind miR-708-5p
197 in the 3'UTR of eGFP on rAAV-hSyn-EGFP. To perform luciferase activity analysis, the
198 wild type and mutated Nnat 3'UTR was inserted into a pmirGLO dual-luciferase
199 expression vector (Promega). Detailed description of the design of these constructs
200 and of the rescue constructs are listed in the supplementary material section. Viral
201 vectors were produced by the Viral Vector Facility (VVF) of the Neuroscience Center
202 Zurich (https://www.vvf.uzh.ch).

203 ## *Animal studies*

204 ## Mouse experiments

205

206 ### *Husbandry, housing, and behavioral testing*

207 All animal experiments on mice were conducted in accordance with Switzerland's
208 animal protection laws and received approval from local cantonal authorities
209 (Approval ID: ZH194/21). Mice were housed collectively in cages designed for 2 to
210 4 individuals, with unrestricted access to food and water. The animal facility
211 maintained an inverted light-dark cycle of 12 hours, with behavioral assessments
212 conducted during the dark phase. Prior to experimentation, mice underwent daily
213 handling lasting 5 minutes each over one week. Details about general behavioral
214 procedures can be found in the supplementary materials and methods section.

Stereotactic surgeries and post-operative care

Stereotactic brain injections were conducted on 2-month-old C57BL/6JRj wild-type mice. The mice were anesthetized with 5% isoflurane in oxygen (1 L/min) and positioned on a stereotactic frame. Viral injections were carried out bilaterally. For dorsal hippocampus, the coordinates used were AP: -2.1mm; ML: ±1.5mm. For ventral hippocampus, the coordinates used were AP: -3.3mm; ML: ±2.7mm. Detailed description of the procedure and post-operative care can be found in the supplementary materials and methods section.

Open Field Test

Mice were placed in an open field box (size: L 45 x W 45 x H 40 cm, TSE System, Bad Homburg, Germany) with a 60-minute exploration window. Dim, yellow light was used in the Open field test of Supplementary Fig. 4H and I, and Supplementary Fig. 6C, D, E. 30 lux, white light was used for the Open Field in Supplementary Fig. 4J. The experiment was recorded, and the TSE VideoMot2 analyzer software (TSE Systems, Bad Homburg, Germany) was used for the automated assessment.

Elevated Plus Maze Test

The mouse was placed on the center of the elevated plus maze, a cross-shaped apparatus with two open arms and two closed arms, each arm measuring L 65 x W 5.5 cm and elevated 62 cm from the ground. 20 lux white light was used. Behavior was recorded on video for five minutes. The videos were automatically analyzed using TSE VideoMot2 analyzer software (TSE Systems, Bad Homburg, Germany)

Saccharin Preference Test

Mice were habituated in their standard group housing to the presence of two bottles for 48 hours before the test. The test was performed by single housing the test animals, and two bottles of tap water or 0.1% Saccharin solution were given to them for 48 hours. The weight of the bottles was recorded at the beginning of the test and every 12 hours around the light change (09:00-09:15 am/pm). The position of the bottle was exchanged each time to avoid side preference. The animals were re-grouped after the test ended.

Novel Object Recognition (NOR) Test

The test was performed as previously described (47), with slight modifications: 1. Twenty-four hours prior to testing, the animals were habituated to the arena used for

247 the test; 2. The break between familiarization and novelty introduction rounds was
248 extended to five minutes or 24 hours.

249 *Marble Burying Test*
250 The test was conducted as previously described (48).

251 *Passive Avoidance Test*
252 The test was conducted using the Passive Avoidance 2-Compartment light-dark
253 arena of the TSE System. The white light was set to 500 lux. On day one, the animal
254 was placed into the light compartment while the door to the dark one wass open
255 and it was allowed to explore; once it passed to the dark compartment, the door
256 closed, and the animal received a 2-seconds foot shock of 0.3 mA after three
257 seconds. On day two, the animal was placed again into the light compartment and,
258 after 15 seconds, the door was automatically opened. The latency to enter the dark
259 compartment was measured.

260 *Tail Suspension Test*
261 The mouse was hung by its tail for a duration of six minutes using a piece of tape
262 affixed to the suspension metal bar, elevated approximately 50 cm from the ground.
263 Before initiating the experiment, a climb-stopper, following the procedure outlined
264 by Can and colleagues(49), was placed at the mouse tail base to prevent climbing.
265 The sessions were recorded on video, and the duration of immobility was
266 subsequently quantified.

267 *Tissue collection*
268 Animals were sacrificed by cervical dislocation and the hippocampus was collected
269 on an ice-cold glass plate and subsequentially snap-frozen for RNA extraction (Trizol
270 protocol) and gene expression analysis or for histological assessments after 4%
271 paraformaldehyde fixation, cryoprotection through 30% sucrose solution, and
272 coronal sectioning at the cryostat. Further details can be found in the supplementary
273 materials and methods section.

274 *Rat experiments*

275 All animal experiments on rats were conducted in accordance with the National
276 Institutes of Health Guidelines for the Care and Use of Laboratory Animals and were
277 subject to prior authorization by the local government (MR 20/35 Nr. 19/2014 and

278 G48/2019; Tierschutzbehörde, Regierungspräsdium Giessen, Germany).
279 Constitutive heterozygous *Cacna1c*$^{+/-}$ animal breeding and the juvenile social
280 isolation paradigm were conducted as described in (22).

281

282 *RT-qPCR*

283 Total RNA extraction from mouse brain tissue, PBMC samples, and primary
284 hippocampal cultures was performed using TRIzol™ Reagent (Thermo Fisher,
285 15596026), and total RNA was subsequently extracted following the manufacturer's
286 guidelines. Further details can be found in the supplementary materials and
287 methods section.

288 *PolyA RNA sequencing sample preparation*

289 Total RNA extraction from mouse hippocampus was extracted TRIzol™ Reagent
290 (Thermo Fisher, 15596026). The RNA was then treated with Turbo DNase enzyme.
291 600 ng of DNase-treated RNA was used for High Throughput Transcriptome
292 sequencing. Libraries were prepared with Illumina TrueSeq mRNA protocol and the
293 transcriptome sequencing was run on Illumina Novaseq 6000. The transcriptome
294 sequencing was carried out by the Functional Genomic Center Zurich (FGCZ,
295 hyperlink: https://fgcz.ch/).

296 *PolyA RNA sequencing analysis*

297 Reads were mapped to the GRCm39 genome with STAR 2.7.8a (50) using the
298 GENCODE M26 annotation as reference and quantified at the gene-level using
299 featureCounts 1.6.4 (51). Genes were filtered using edgeR's filterByExpr function
300 before differential expression analysis with edgeR 3.32.1 (52) using likelihood ratio
301 tests with 3 surrogate variables estimated using sva 3.38.0 (53). TargetScan 7 (54)was
302 used to predict miRNA targets. For gene expression across different brain cell types
303 (Figure 4B), the Allen 10X+smartSeq taxonomy and per-cluster expression was used,
304 aggregating non-neuronal cell types into broader classes.

305 *Western blot*

306 Proteins from primary hippocampal neurons were isolated using ice cold RIPA lysis
307 buffer. 20ug of protein was mixed with 4xLaemmli Sample Buffer (Biorad) and were
308 run on a 4–20% Mini-PROTEAN® TGX™ Precast Protein Gels (Biorad). Proteins were

309 transferred on a nitrocellulose membrane and blocked for two hours at room
310 temperature in blocking solution and incubated in primary antibody solution for 48
311 hours at 4°C. Membranes were washed and incubated with secondary antibody for
312 1h. Membranes were washed five times in TBS-T, developed with the Clarity™
313 Western ECL Substrate (Bio-Rad) and visualized with the ChemiDocTM MP, Imaging
314 System (BioRad). Further details can be found in the supplementary materials and
315 methods section.

316 *Statistical analysis*

317 Details regarding the statistical analysis are listed in the Supplementary Materials
318 and methods section.

319 Results

320

321 *miR-708-5p is upregulated in the peripheral blood of human*
322 *subjects at risk for or diagnosed with MDs.*

323
324 miRNAs have been associated with MDs, but their functional role in the development
325 of such disorders is still largely unexplored (14). To identify candidate miRNAs, we
326 performed small-RNA sequencing with total RNA obtained from peripheral blood
327 mononuclear cells (PBMCs) of healthy subjects (n=52) from the FOR2107 cohort (39)
328 characterized by a high genetic (at least one first degree relative diagnosed with a
329 mood disorder; GR group; n=14) or environmental (ER group; childhood trauma
330 based on childhood trauma questionnaire (CTQ) score; n=16) predisposition to
331 develop MDs (Fig. 1A; Table 1). For this initial analysis, we selected females since we
332 were able to form more homogeneous GR and ER groups with females compared
333 to males. We then focused on miRNAs that were differentially expressed in both ER
334 and GR compared to healthy control subjects (CTL group; no known genetic or
335 environmental risk factors; n=18), reasoning that such miRNAs would represent
336 strong candidates for being functionally involved in MDs. We found that a total of six
337 miRNAs (miR-412-5p, miR-100-5p, miR-501-3p, miR-642a-5p, miR-4999-5p, miR-
338 708-5p) fulfilled this criterium (Fig. 1B and C). Among them miR-708-5p was of
339 specific interest, since it was the most strongly upregulated miRNA. It was previously

340 shown to be induced by various forms of cellular stress (26–30) and had been
341 associated with BD in the past (21). We could confirm that miR-708-5p is significantly
342 upregulated in the GR and ER groups using qPCR (Fig. 1D).

343 Given these results, we speculated that miR-708-5p could also be altered in PBMCs
344 of patients diagnosed with MDD or BD. Therefore, we assessed the levels of miR-
345 708-5p in PBMCs obtained from MDD (n=42) and BD (n=63) patients (Fig. 1A; Table
346 1) by qPCR. miR-708-5p was significantly upregulated in female BD (n=26) and MDD
347 (n=18) patients (Fig. 1E) compared to CTL (n=26), after correcting for age and
348 antidepressant treatment (Fig. S1A-B), whereby the effect was more pronounced in
349 BD compared to MDD patients. A similar picture was observed in male patients.
350 Here, the increase was highly significant for BD subjects (Fig. 1F), after age and
351 antidepressant treatment correction (Fig. S1C), and only trending for patients
352 affected by MDD (Fig. 1F, Fig. S1D). Furthermore, miR-708-5p was significantly
353 upregulated in both subtypes of BD in both female (Fig. S1E) and male (Fig. S1F)
354 subjects. In female subjects, the only significant BD state for miR-708-5p
355 upregulation was mania, although it only included two samples (Fig. S1G). There was
356 also a significant miR-708-5p upregulation in depressive and hypomanic states in
357 male subjects (Fig. S1H).

358 miR-708-5p levels showed a trending positive correlation with the Young Mania
359 Rating Scale (YMRS), which is used to assess manic-like symptomatology in subjects
360 affected by BD (Fig. 1G). In contrast, miR-708-5p did not show any correlation with
361 YMRS in female subjects affected by BD (Fig. 1H). We also investigated whether miR-
362 708-5p correlated with the Beck's depression inventory (BDI), in MDD male and
363 female subjects, but no significant or trending correlation could be observed (Fig.
364 S1I and J). Taken together, our results suggest that miR-708-5p is elevated in the
365 peripheral blood of mood disorder patients, with a particularly strong upregulation
366 observed for BD males.

367 We then asked if miR-708-5p was also differentially expressed in PBMCs obtained
368 from patients suffering from related psychiatric disorders. For that purpose, we
369 chose schizophrenia (SCZ), given the high genetic similarities between SCZ and BD
370 (55). We performed qPCR on PBMCs from female (n=8) and male (n=15) SCZ

371 patients but were unable to detect any significant change in miR-708-5p expression
372 compared to healthy control subjects (CTL; n=19) (Fig. S1K).

373 One of the biggest challenges in mood disorder diagnostics is to distinguish BD and
374 MDD patients, especially when BD patients are in a depressive phase (56,57). Given
375 our results from Fig. 1D-H, we hypothesized that miR-708-5p expression in PBMCs
376 could be used as a diagnostic tool to classify samples into BD or control group, and
377 BD or Control and MDD group. To do this, we performed receiver operating
378 characteristic (ROC) curve analysis (58) and used miR-708-5p expression as
379 predictor variable. We found that miR-708-5p alone performed better in male
380 samples than in female samples when asked to discriminate BD patients from
381 controls and MDD patients (Fig S2A and B), consistent with our previous results (Fig.
382 1 D-H). We then performed the same analysis using the expression values of miR-
383 499a-5p, which we previously found to be significantly upregulated in male BD
384 subjects compared to healthy controls (22). Like miR-708-5p, miR-499a-5p
385 performed better as a classifier in male subjects compared to female subjects (Fig
386 S2C and D). Furthermore, we performed another ROC curve analysis considering
387 both miRNAs together and found that the combined expression of miR-708-5p and
388 miR-499a-5p performs better (AUC=0.908) in classifying male BD vs controls and
389 MDD (Fig. 1I) than when the miRNAs are analyzed individually. In addition, the
390 combination performs better (AUC=0.914) also in classifying male BD vs controls
391 (AUC=0.914) (Fig S2E).

392 Taken together, our results show that the combined expression of miR-708-5p and
393 miR-499a-5p in PBMCs shows a good predictive potential to distinguish BD patients
394 from MDD patients and healthy controls, in particular regarding males.

395

396 *miR-708-5p is expressed in rat hippocampal neurons and*
397 *upregulated in the hippocampus of rat models of*
398 *environmental or genetic risk for MDs.*
399

400 To further study the functional role of miR-708-5p in MDs, we considered rodents
401 given their extensive use in modelling psychiatric conditions (59). As a first step, we

402 investigated whether miR-708-5p was expressed in different regions of the rat brain
403 (Fig. 2A). We observed robust expression in regions classically implicated in MDs
404 and cognitive function, such as the amygdala, frontal cortex, and hippocampus (Fig.
405 2A). Next, we assessed miR-708-5p expression in rat hippocampal primary neurons.
406 Single-molecule fluorescence *in situ* hybridization (sm-FISH) showed that miR-708-
407 5p is expressed in both CamK2a+ excitatory and GAD2+ inhibitory neurons in rat
408 hippocampal cultures, illustrating its widespread neuronal distribution (Fig. 2B and
409 2C). miR-708-5p expression in rat hippocampal cultures decreased over time during
410 *in vitro* development, indicating a role for miR-708-5p at early stages of neuronal
411 development (Fig. 2D). Motivated by the findings of miR-708-5p elevation in
412 peripheral blood of humans at risk to develop MDs (Fig. 1B-D), we asked whether
413 miR-708-5p was similarly dysregulated in rat genetic and environmental models of
414 MDs. As a genetic model, we chose rats heterozygous for *Cacna1c* (*Cacna1c*$^{+/-}$*),* a
415 repeatedly validated cross-disorder psychiatric risk gene (60–65). Environmental risk
416 was modelled by juvenile social isolation, a widely recognized model for early life
417 trauma, e.g., childhood maltreatment (66) (Fig. 2E). miR-708-5p was significantly
418 upregulated by social isolation in the hippocampus of juvenile wild-type rats
419 compared to their group-housed counterparts (Fig. 2F), indicating parallels between
420 the early life stress-related modulation of miR-708-5p expression in human
421 peripheral blood and rat brain. Furthermore, *Cacna1c* heterozygosity led to an
422 upregulation of miR-708-5p in the rat hippocampus independent of social housing
423 conditions, suggesting that, like our human PBMC data (Fig. 1C-D), a *genetic*
424 predisposition for MDs is sufficient to induce miR-708-5p expression in the rat brain
425 (Fig. 2F). Our comprehensive analysis across various experimental paradigms
426 revealed that miR-708-5p expression is linked to both environmental stressors and
427 genetic factors associated with MDs in both humans and rodents. Therefore,
428 manipulation of miR-708-5p in the rodent brain represents a viable strategy to study
429 the involvement of miR-708-5p in the development of mood disorder-associated
430 endophenotypes as well as the underlying molecular mechanisms.

431

432 ## *miR-708-5p overexpression in the mouse hippocampus*
433 ## *recapitulates BD-associated endophenotypes.*
434

435 We next investigated whether stress-induced upregulation of miR-708-5p in the
436 rodent hippocampus is causally involved in the development of mood disorder-
437 associated behavioral endophenotypes. Towards this end, miR-708-5p was
438 ectopically overexpressed in the mouse hippocampus using stereotactic injection of
439 a recombinant rAAV expressing a miR-708-5p hairpin (hp) under the control of the
440 human synapsin (hSYN) promoter (Fig. S3A). To ensure the functionality of the
441 overexpressing construct, we performed luciferase assay upon transfection of miR-
442 708-5p overexpressing plasmid (hp708-p) together with a luciferase sensor
443 harboring two perfect binding sites for miR-708-5p. Thereby, we detected a
444 significant decrease in luciferase activity upon miR-708-5p overexpression
445 compared to the control (hpCTL-p) (Fig. S3B), demonstrating efficient repression of
446 the reporter gene by the overexpressed miR-708-5p. We went on to perform
447 stereotactic surgeries on seven to eight-week-old mice, which then underwent a
448 four-week recovery period before behavioral assessments were conducted (Fig. 3A).
449 Our approach led to a widespread infection of both the dorsal and ventral
450 hippocampus (Fig. 3B), as well as to a robust miR-708-5p overexpression compared
451 to control infected mice (Fig. 3C; Suppl. Fig. 3C-E). . Male mice overexpressing miR-
452 708-5p in the hippocampus exhibited a significant decrease in immobility during the
453 tail suspension test (TST), indicative of reduced behavioral despair, while this effect
454 was not observed in female mice (Fig. 3D-E). Interestingly, neither male nor female
455 mice with miR-708-5p overexpression showed significant differences in saccharin
456 preference compared to control groups, suggesting no alteration in anhedonia-like
457 behavior (Fig. S3F-G). Furthermore, we observed a strong, although non-significant
458 trend, for elevated anxiety-related compulsive behavior, as assessed by the marble
459 burying test (MBT), in miR-708-5p overexpressing male mice (Fig. 3F). However,
460 results from the elevated plus maze (EPM) did not reveal significant changes in
461 general anxiety levels between the experimental groups (Suppl. Fig 3 H-I). We
462 further evaluated cognitive functions since cognitive impairments are frequently
463 observed in mood disorder patients. Our results from the novel object recognition

464 (NOR) (Fig. 3G) test revealed that miR-708-5p overexpression led to a significant
465 impairment in object recognition memory after a 24-hour delay specifically in male
466 mice (Fig. 3H; Fig. S4A, B). This impairment was also evident in short-term memory
467 (5 min delay), as miR-708-5p overexpressing mice failed to discriminate between
468 familiar and novel objects after a brief five-minute interval, this time in a sex-
469 independent manner (Fig. 3 I, J; Fig. S4C-F). Passive avoidance, however, was intact
470 in miR-708-5p expressing male mice (Fig. S4G). Locomotor activity, assessed
471 through the OFT remained unchanged, ruling out locomotion as a confounding
472 factor in our behavioral assessments (Fig. S4H-J). Together, our results provide
473 strong evidence that hippocampal overexpression of miR-708-5p leads to distinct
474 mood disorder-associated behaviors. Specifically, reduced behavioral despair,
475 elevated compulsive behavior and impaired recognition memory are consistent with
476 a role for miR-708-5p in the etiology of BD, which aligns with our results from
477 expression analysis in mood disorder patients (Fig. 1). Interestingly, miR-708-5p
478 peripheral expression in human subjects negatively correlated with the score from
479 the D2 attention test (Fig. 3K, S4K and L) in both female and male subjects, further
480 suggesting a role for miR-708-5p in human cognitive processes associated with BD.

481 *miR-708-5p directly targets Neuronatin (Nnat), an ER-*
482 *resident protein involved in calcium homeostasis.*
483

484 As a next step, we decided to explore the mechanisms underlying miR-708-5p
485 dependent regulation of BD-associated behavior. miRNAs regulate gene expression
486 through binding to mRNAs, predominantly leading to their degradation or inhibition
487 of translation (15). Therefore, we reasoned that the analysis of the hippocampal
488 transcriptome of miR-708-5p overexpressing mice could inform us about potential
489 miR-708-5p downstream targets mediating behavioral effects. polyA-RNA-
490 sequencing (seq) revealed 118 differentially expressed genes (DEG) (p-value<0.01;
491 FDR<0.001) between the hippocampus of hp-708 and hp-control infected mice (Fig.
492 4A). Sixteen DEGs were significantly downregulated and contained predicted miR-
493 708-5p binding sites (Fig. 4B), making them strong candidates for direct targets of
494 miR-708-5p. Nnat was of particular interest, since it has been previously identified as
495 a direct target of miR-708-5p (27,33) and its 3'UTR contains a miR-708-5p perfect

496 binding site (Fig. 4C). The Nnat gene encodes for a small ER-resident protein which
497 acts as an endogenous inhibitor of the SERCA calcium pump, thereby controlling
498 intracellular calcium homeostasis which is disturbed in BD (38). Moreover, within the
499 mouse brain, Nnat is primarily expressed in glutamatergic CA1 and CA3 neurons
500 based on published single cell RNA-seq data (Fig. 4B), consistent with a functional
501 interaction of miR-708-5p and Nnat in neurons. To further validate our RNA-seq data,
502 we measured the levels of Nnat mRNA in the hippocampus of mice upon miR-708-
503 5p overexpression (Fig. 4D) and detected a significant decrease compared to
504 control infected mice (Fig. 4E). So far, our expression analysis on hippocampal tissue
505 did not allow to distinguish between effects occurring in neuronal and non-neuronal
506 cells. Therefore, we further extended our analysis to rat primary hippocampal neuron
507 cultures. Like in the *in vivo* experiments, infection of rat neurons with hp708 resulted
508 in a robust upregulation of miR-708-5p levels (Fig. 4F) and led to significant
509 reductions in Nnat mRNA (Fig. 4G), and protein levels (Fig.4H and I), demonstrating
510 that miR-708-5p represses endogenous Nnat expression in neurons. To prove that
511 the downregulation of Nnat is due to a direct interaction of the miR-708-5p and Nnat
512 mRNA via the predicted miR-708-5p binding site, we performed luciferase reporter
513 gene assay in primary rat hippocampal neurons. Luciferase reporter genes were
514 either fused to the wild type 3'UTR of Nnat (Nnat wt) or to a 3'UTR of Nnat containing
515 several point mutations expected to prevent miR-708-5p binding (Nnat mt).
516 Whereas Nnat wt was efficiently downregulated by co-transfection of hp708-p, Nnat
517 mt was insensitive to miR-708-5p overexpression (Fig. 4J). The results obtained from
518 these assays therefore confirm that miR-708-5p directly suppresses Nnat expression
519 through a 3'UTR interaction. In a complementary approach, we employed a target-
520 directed miRNA degradation (TDMD) construct (sp708-p) to reduce endogenous
521 miR-708-5p levels (Fig. S5A-C). Here, we detected a significant increase in luciferase
522 activity upon transfection with sp708-p compared to control for Nnat wt, but not
523 Nnat mt expressing neurons (Fig. 4K). In summary, our results from RNA-seq, qPCR
524 and luciferase assays establish Nnat as a direct target of miR-708-5p in rodent
525 hippocampal neurons.

526 ## *Restoring Nnat expression in miR-708-5p overexpressing*
527 *hippocampal neurons rescues BD-associated behavioral*
528 *endophenotypes in mice.*
529

530 Building upon our identification of Nnat as a potential regulatory target of miR-708-
531 5p in the hippocampus, we hypothesized that Nnat downregulation might underlie
532 the observed BD-associated behavioral alterations elicited by miR-708-5p
533 overexpression. To test this hypothesis, we engineered a construct which allows to
534 simultaneously overexpress Nnat and miR-708-5p upon viral infection. This was
535 achieved by inserting the coding sequence of Nnat downstream of the hSYN
536 promoter, coupled with a P2A self-cleaving peptide; this fragment was followed by
537 the EGFP coding sequence and the overexpressing miR-708-5p hairpin. As a control,
538 we utilized a similar construct where the mCherry coding sequence replaced Nnat
539 followed by EGFP and hp708 or EGFP and hpCTL (Fig 5A). rAAV obtained from
540 these constructs was injected into the hippocampus of seven/eight weeks old male
541 mice by stereotaxis, followed by a four-week recovery period before behavioral
542 assessments as described in Fig. 3A. Expression analyses confirmed the
543 upregulation of miR-708-5p and the intended modulation of Nnat levels (Fig. 5B, 5C;
544 Suppl. Fig 6A, and Fig. 5D, Suppl. Fig 6B). Notably, the mCherry-P2A-hp708
545 construct led to a pronounced upregulation of miR-708-5p (Fig. 5B) and a
546 corresponding decrease in Nnat levels, as opposed to the control and the Nnat-P2A-
547 hp708 conditions, the latter of which restored Nnat expression to wild-type levels
548 (Fig. 5C and Suppl. Fig 6A, B). Behavioral analyses revealed that miR-708-5p
549 overexpression alone impaired object discrimination ability in the NOR test as
550 expected (Fig. 5D, Suppl. Fig. 6F). This was not observed in mice injected with the
551 Nnat-P2A-hp708 construct, which displayed a restoration of exploratory behavior
552 towards the novel object to a similar degree than control injected mice (Fig. 5D,
553 Suppl. Fig. 6F). Furthermore, as expected from our previous results, the total
554 exploration time of the animals was not affected in any of the conditions (Suppl. Fig
555 6G). Similarly, the TST results indicated reduced behavioral despair in miR-708-5p
556 overexpressing mice, an effect that was normalized upon co-expression of Nnat,
557 again mirroring control group behaviors (Fig. 5E). Furthermore, no significant

558 differences between experimental groups were observed in locomotor activity in the
559 OFT (Suppl. Fig. 6C-E). Taken together, our results strongly suggest that Nnat is an
560 important downstream target in mediating the effects on BD-associated behavioral
561 endophenotypes caused by miR-708-5p overexpression in the hippocampus.

562

563 # Discussion

564 In this study, we found that miR-708-5p is upregulated in healthy human subjects at
565 high risk to develop MDs, in MD patients and in genetic and environmental rat MD
566 models. Furthermore, peripheral miR-708-5p expression was negatively correlated
567 with scores from the D2 attention test. Moreover, miR-708-5p overexpression in the
568 mouse hippocampus led to memory impairments, increased compulsive anxiety
569 and reduced depression-like behavior. Together with the fact that miR-708-5p was
570 nominally associated with BD in a previous GWAS (21), our results strongly implicate
571 this miRNA in the etiology of BD and suggest its potential use as BD biomarker.

572 **miR-708-5p function in BD-associated behaviors**

573 Modelling the complex symptomatology of BD in animal models is challenging and
574 has so far only been partially achieved in mice in the context of miRNA manipulation.
575 For example, the acute manipulation of miR-124 in the PFC of mice led to impaired
576 social behavior and locomotor disturbances upon injection of psychostimulants (67).
577 The hippocampal overexpression of miR-499-5p in *Cacna1c*$^{+/-}$ rats provoked
578 memory impairments, recapitulating the cognitive deficits encountered in BD (22)
579 which include difficulties in attention, memory and executive functions present
580 during the different mood phases and during remission (68). Accordingly, we found
581 that in humans miR-708-5p peripheral expression is negatively correlated with D2
582 scoring in the attention test (69). Moreover, we found that both female and male
583 mice overexpressing miR-708-5p in the hippocampus showed memory
584 impairments. Furthermore, male, but not female, mice showed significantly
585 decreased immobility in the TST. This test has been historically used to test
586 antidepressant effects on mice but is also employed in mouse models of manic
587 behavior. For example, BD mouse models of mania (Ankyrin-G conditional knockout,

588 Clock19 deficient mice) show reduced immobility during TST (11) and the FST (10),
589 suggesting that the reduced behavioral despair in our model could reflect a function
590 of miR-708-5p in manic-like behavior. This is further supported by increased
591 (although non-significant) marble burying, indicative of a compulsive response to
592 anxiogenic stimuli. However, in our study, the antidepressant-like behavior was
593 neither accompanied by increased exploratory behavior in the OFT, nor increased
594 risk-taking during EPM testing, both of which are usually observed in mouse models
595 of mania. We consider two possible explanations for this discrepancy. First, contrary
596 to most of the models reported in the literature, our animal model is characterized
597 by an acute and selective overexpression of miR-708-5p in the hippocampus.
598 Therefore, we might expect to observe endophenotypes dependent on the
599 hippocampus (e.g., antidepressant-like behavior, cognition), but not those related
600 to other brain regions, such as the amygdala, prefrontal cortex, or cerebellum (e.g.,
601 risk-taking behavior, hyperactivity). Alternatively, the miR-708-5p/Nnat pathway
602 might selectively control specific aspects of manic- and depression-like behavior. To
603 distinguish between these possibilities, it will be important to study the role of miR-
604 708-5p overexpression in other brain areas relevant for BD-associated behaviors in
605 the future.

606 **Role of miR-708-5p in excitatory vs. inhibitory neurons**

607 The balance between excitation and inhibition in neuronal network activity is
608 disrupted in many neuropsychiatric disorders, including MDD (70), BD, and SCZ (71–
609 73). In this regard, inhibitory neuron dysfunction is increasingly considered in MDs.
610 Our approach to overexpress miR-708-5p in the hippocampus using a pan-neuronal
611 promoter (Synapsin-1) does not allow to distinguish the contribution of defects in
612 excitatory and inhibitory neurons to the observed phenotypes. Based on published
613 Ago pull-down and single cell RNA-seq datasets, Nnat is primarily expressed in
614 excitatory neurons (32). In contrast, Nnat was found to be upregulated in
615 parvalbumin-positive (PV+) interneurons of the hippocampus and amygdala in an
616 Angelman Syndrome mouse model (33), as well as in human PV+ interneurons from
617 Lafora Disease patients (74). Hence, the role of miR-708-5p in excitatory and
618 inhibitory neuron populations needs to be further investigated by cell-specific
619 overexpression of miR-708-5p followed by BD-related behavioral characterization.

620 **miR-708-5p regulation by genetic and environmental risk factors**

621 BD has the highest rate of inheritance among psychiatric disorders (up to 70%).
622 However, genetics alone cannot explain the degree at which BD is inherited in
623 families, suggesting that environmental factors need to be considered as well
624 (2,75,76). Childhood maltreatment is the most studied environmental stressor in the
625 context of MDs (3,5,77). Interestingly miR-708-5p was upregulated in the juvenile
626 social isolation rat model, an animal model for childhood maltreatment (78).
627 Consistent with this result, a recent study reported miR-708-5p upregulation in the
628 PFC upon seven days of chronic social defeat in vulnerable rats compared to resilient
629 animals (31). Moreover, miR-708-5p levels are elevated in *Cacna1c*$^{+/-}$ rats, a well-
630 established genetic model of psychiatric disorders (79), even without environmental
631 stressors. Taken together, these results suggest that genetic and environmental risk
632 might impinge on common pathways triggering miR-708-5p expression.
633 Furthermore, studies in the context of ovarian cancer revealed the presence of a
634 glucocorticoid response element upstream of *ODZ4* (29), suggesting that the
635 expression of the host gene and of miR-708-5p might be responsive to
636 glucocorticoids (80). Moreover, studies in the context of ER stress suggest that miR-
637 708-5p expression is induced by CHOP, a transcription factor involved in the
638 Unfolded Protein Response (UPR) upon ER stress (30). Furthermore, metformin-
639 induced upregulation of miR-708-5p elicits Nnat downregulation in prostate cancer,
640 leading to the expression of ER-Stress-mediators. Finally, bisphenol A, an ubiquitous
641 endocrine disruptive chemical, induces miR-708-5p in hypothalamic neurons in a
642 CHOP-dependent manner, accompanied by Nnat downregulation (26). Thus, we
643 speculate that increased ER stress, which has been implicated in BD, is a critical
644 mediator of miR-708-5p upregulation in response to genetic and environmental
645 stress in neurons.

646 **Molecular and cellular mechanisms downstream of the miR-708-5p/Nnat**
647 **interaction**

648 Dysregulated calcium homeostasis has been previously implicated in the
649 pathophysiology of BD (38). Our results from this and a previous study (22) are
650 consistent with disrupted calcium flux via L-type calcium channels, e.g., due to

651 *Cacna1c* mutation, as a major underlying cause. However, ER calcium dynamics
652 emerges as another major player. For example, store operated calcium entry (SOCE)
653 is dysregulated in BD-induced pluripotent stem cells, leading to earlier neuronal
654 differentiation and abnormal neurite outgrowth (81). Furthermore**,** altered
655 expression of the miR-708-5p target Nnat has been associated with defective
656 intracellular and ER calcium levels (33,74,82). Nnat is a small ER membrane protein
657 which acts as an antagonist of the sarco-endoplasmic reticulum calcium ATPase
658 (SERCA) pump, thereby interfering with calcium re-uptake into the ER (35,36).
659 Consistently, it has been reported that miR-708-5p-mediated downregulation of
660 Nnat causes lower basal cytoplasmic calcium levels (33). On the other hand,
661 excessive ER calcium re-uptake could result in ER calcium overload, which in turn
662 leads to calcium leakage to the cytoplasm and mitochondria (83,84), with negative
663 consequences for calcium signaling and cell health, as exemplified in Alzheimer's
664 disease (85,86). Clearly, further studies are warranted on the impact of aberrant miR-
665 708-5p/Nnat signaling on intraneuronal calcium homeostasis in the context of BD.

666 **miR-708-5p as a potential biomarker in BD**

667 Our findings indicate an upregulation of miR-708-5p in PBMCs of females at risk of
668 MDs and in patients with MDD and BD. A previous study reported a downregulated
669 expression of miR-708-5p in leukocytes of women in depressive state compared to
670 women in remission (87). These results are in line with our detected expression
671 difference between female euthymic patients and depressive patients. For male
672 samples, on the other hand, our data suggest a role of miR-708-5p specifically in the
673 manic phase of the disorder, as indicated from the YMRS correlation and the
674 behavioral characterization. Although SCZ and BD were reported to have the highest
675 genetic correlation among psychiatric disorders (77), we found that miR-708-5p
676 expression was unchanged in peripheral samples of patients diagnosed with SCZ.
677 This suggests a rather specific expression pattern of miR-708-5p in the spectrum of
678 MDs. Within MDs, miR-708-5p upregulation was most pronounced in BD. This is
679 impressively illustrated by our ROC curve analysis, which shows that miR-708-5p
680 expression, when combined with miR-499-5p, effectively distinguishes BD patients
681 not only from healthy controls, but also from MDD patients. Although miR-708-5p is
682 significantly upregulated in both male and female BD patient samples, the degree

683 of increase is higher in males compared to females (8.8-fold vs. 4.23-fold change).
684 Moreover, based on our ROC curve analysis, miR-708-5p expression discriminated
685 male BD patients better from control and MDD compared to female patients.
686 Together, these observations suggest a potential sex-specific role of miR-708-5p in
687 BD, which also aligns with our results from mouse behavior. Sex differences in BD
688 manifest across various aspects, ranging from clinical symptoms to the progression
689 of the disorder. Males typically encounter their first manic episode at a younger age
690 compared to females, who are more likely to experience a depressive episode at the
691 onset of BD (6). In contrast, females experience a higher incidence of depressive
692 episodes and hypomania, leading to a more frequent diagnosis of BD type II (88).
693 Females are also more susceptible to mixed episodes(89), rapid cycling of mood
694 phases (90,91), and show a greater likelihood of attempting suicide (92). Whereas
695 men perform better in working memory tasks, females performed better in verbal
696 learning and memory task recognition (8). In this regard, miRNAs have been
697 previously implicated in SCZ/BD differential regulations of circadian, cholinergic,
698 and neurokine pathways (93).

699 We propose that miR-708-5p represents a promising candidate for the development
700 of a biomarker that helps to stratify mood disorder patients based on disease entity,
701 specific phases of the disease and sex, which should greatly help with diagnosis and
702 therapy.

703

704 # Acknowledgements

705 We greatly acknowledge the technical support in the preparation of primary
706 hippocampal cultures by Cristina Furler, Tatjana Wüst and Dr. Roberto Fiore. We also
707 thank Dr. Brunno Rocha Levone for support in behavioral testing and inputs on the
708 manuscript. We also thank Darren Kelly for support in designing the TDMD
709 construct, and David Colameo and Emanuel Sonder for support in the statistical
710 analysis. RNA sequencing was performed at the Functional Genomics Center Zurich
711 (FGCZ) of the University Zurich and ETH Zurich. The work in the lab of GS was
712 supported by grants from ETH Zurich (ETH-24 18-2 Grant (NeuroSno)) and the Swiss
713 National Science Foundation (SNSF 310030E_179651, 32NE30_189486,

310030_205064/1). This work was further funded by the German Research Foundation (DFG grants FOR2107 KI588/14-1, and KI588/14-2, and KI588/20-1, KI588/22-1 to TK; grant FOR2107 DA1151/5-1, DA1151/5-2, DA1151/9-1, DA1151/10-1, DA1151/11-1 to UD; grant FOR2107 SCHR 1136/3-1 to GS; grant DFG WO 1732/4-1 and DFG WO 1732/4-2 to MW; grant DFG 559/14-1 and DFG 559/14-2 to RS), as well as the Fonds Wetenschappelijk Onderzoek – Vlaanderen (FWO; Research Foundation – Flanders) through a senior project to MW (G0C0522N), and the Interdisciplinary Center for Clinical Research (IZKF) of the medical faculty of Münster (grant Dan3/022/22 to UD). Biosamples and corresponding data were sampled, processed, and stored in the Marburg Biobank CBBMR.

Author contributions

Carlotta Gilardi: Investigation; writing. Helena Martins: Investigation. Pierre-Luc Germain: Formal analysis. Fridolin Gross: Formal analysis. Alessandra Lo Bianco: Investigation. Silvia Bicker: Investigation; methodology. Ayse Özge Sungur: Investigation. Theresa M. Kisko: Investigation. Rainer K.W. Schwarting: Supervision. Frederike Stein: Data curation; formal analysis. Susanne Meinert: Data curation. Udo Dannlowski: supervision. Tilo Kircher: supervision; project administration. Markus Wöhr: supervision; project administration. Gerhard Schratt: Conceptualization; supervision; writing.

Conflict of Interest

The authors declare that they have no conflict of interest.

Data availability

RNA sequencing data has been deposited to Gene Expression Omnibus (GEO, small RNA-sequencing Fig. 1B-C, accession numbers: GSE261287; RNA-sequencing Fig. 4A, accession numbers: GSE261288).

Bibliography

1. McGuffin P, Rijsdijk F, Andrew M, Sham P, Katz R, Cardno A. The Heritability of Bipolar Affective Disorder and the Genetic Relationship to Unipolar Depression. Arch Gen Psychiatry. 2003 May 1;60(5):497.

2. Craddock N, Sklar P. Genetics of bipolar disorder. The Lancet. 2013 May;381(9878):1654–62.

3. Rodriguez V, Alameda L, Trotta G, Spinazzola E, Marino P, Matheson SL, et al. Environmental Risk Factors in Bipolar Disorder and Psychotic Depression: A Systematic Review and Meta-Analysis of Prospective Studies. Schizophr Bull. 2021 Jul 8;47(4):959–74.

4. Nemeroff CB. Paradise Lost: The Neurobiological and Clinical Consequences of Child Abuse and Neglect. Neuron. 2016 Mar;89(5):892–909.

5. Aas M, Bellivier F, Bettella F, Henry C, Gard S, Kahn J-P, et al. Childhood maltreatment and polygenic risk in bipolar disorders. Bipolar Disord. 2020;22(2):174–81.

6. Kennedy N, Everitt B, Boydell J, Os JV, Jones PB, Murray RM. Incidence and distribution of first-episode mania by age: results from a 35-year study. Psychol Med. 2005 Jun;35(6):855–63.

7. Zhang L, Swaab DF. Sex differences in bipolar disorder: The dorsolateral prefrontal cortex as an etiopathogenic region. Front Neuroendocrinol. 2024 Jan 1;72:101115.

8. Arnold LM. Gender differences in bipolar disorder. Psychiatr Clin North Am. 2003 Sep 1;26(3):595–620.

9. Li X, Chen B, Zhang D, Wang S, Feng Y, Wu X, et al. A novel murine model of mania. Mol Psychiatry. 2023 Jul;28(7):3044–54.

10. Roybal K, Theobold D, Graham A, DiNieri JA, Russo SJ, Krishnan V, et al. Mania-like behavior induced by disruption of CLOCK. Proc Natl Acad Sci. 2007 Apr 10;104(15):6406–11.

11. Zhu S, Cordner ZA, Xiong J, Chiu C-T, Artola A, Zuo Y, et al. Genetic disruption of ankyrin-G in adult mouse forebrain causes cortical synapse alteration and behavior reminiscent of bipolar disorder. Proc Natl Acad Sci. 2017 Sep 26;114(39):10479–84.

12. Kozikowski AP, Gaisina IN, Yuan H, Petukhov PA, Blond SY, Fedolak A, et al. Structure-Based Design Leads to the Identification of Lithium Mimetics That Block Mania-like Effects in Rodents. Possible New GSK-3β Therapies for Bipolar Disorders. J Am Chem Soc. 2007 Jul 1;129(26):8328–32.

13. Dao DT, Mahon PB, Cai X, Kovacsics CE, Blackwell RA, Arad M, et al. Mood Disorder Susceptibility Gene CACNA1C Modifies Mood-Related Behaviors in Mice and Interacts with Sex to Influence Behavior in Mice and Diagnosis in Humans. Biol Psychiatry. 2010 Nov 1;68(9):801–10.

14. Martins HC, Schratt G. MicroRNA-dependent control of neuroplasticity in affective disorders. Transl Psychiatry. 2021 May 3;11(1):263.

15. Bartel DP. Metazoan MicroRNAs. Cell. 2018 Mar;173(1):20–51.

16. Schratt G. microRNAs at the synapse. Nat Rev Neurosci. 2009 Dec;10(12):842–9.

17. Emde A, Hornstein E. miRNAs at the interface of cellular stress and disease. EMBO J. 2014 Jul;33(13):1428–37.

18. Moreau MP, Bruse SE, David-Rus R, Buyske S, Brzustowicz LM. Altered microRNA expression profiles in post-mortem brain samples from individuals with schizophrenia and bipolar disorder. Biol Psychiatry. 2011 Jan 15;69(2):188–93.

19. Zhang Z, Convertini P, Shen M, Xu X, Lemoine F, de la Grange P, et al. Valproic Acid Causes Proteasomal Degradation of DICER and Influences miRNA Expression. Pfeffer S, editor. PLoS ONE. 2013 Dec 17;8(12):e82895.

20. Coradduzza D, Garroni G, Congiargiu A, Balzano F, Cruciani S, Sedda S, et al. MicroRNAs, Stem Cells in Bipolar Disorder, and Lithium Therapeutic Approach. Int J Mol Sci. 2022 Jan;23(18):10489.

21. Forstner AJ, Hofmann A, Maaser A, Sumer S, Khudayberdiev S, Mühleisen TW, et al. Genome-wide analysis implicates microRNAs and their target genes in the development of bipolar disorder. Transl Psychiatry. 2015 Nov 10;5(11):e678–e678.

22. Martins HC, Gilardi C, Sungur AÖ, Winterer J, Pelzl MA, Bicker S, et al. Bipolar-associated miR-499-5p controls neuroplasticity by downregulating the Cav1.2 subunit CACNB2. EMBO Rep. 2022 Oct 6;23(10):e54420.

23. He S, Liu X, Jiang K, Peng D, Hong W, Fang Y, et al. Alterations of microRNA-124 expression in peripheral blood mononuclear cells in pre- and post-treatment patients with major depressive disorder. J Psychiatr Res. 2016 Jul;78:65–71.

24. Liu S, Zhang F, Shugart YY, Yang L, Li X, Liu Z, et al. The early growth response protein 1-miR-30a-5p-neurogenic differentiation factor 1 axis as a novel biomarker for schizophrenia diagnosis and treatment monitoring. Transl Psychiatry. 2017 Jan 10;7(1):e998–e998.

816 25. Psychiatric GWAS Consortium Bipolar Disorder Working Group, Sklar P, Ripke
817 S, Scott LJ, Andreassen OA, Cichon S, et al. Large-scale genome-wide
818 association analysis of bipolar disorder identifies a new susceptibility locus near
819 ODZ4. Nat Genet. 2011 Oct;43(10):977–83.

820 26. McIlwraith EK, Lieu CV, Belsham DD. Bisphenol A induces miR-708-5p through
821 an ER stress-mediated mechanism altering neuronatin and neuropeptide Y
822 expression in hypothalamic neuronal models. Mol Cell Endocrinol. 2022 Jan
823 1;539:111480.

824 27. Yang J, Wei J, Wu Y, Wang Z, Guo Y, Lee P, et al. Metformin induces ER stress-
825 dependent apoptosis through miR-708-5p/NNAT pathway in prostate cancer.
826 Oncogenesis. 2015 Jun 15;4(6):e158–e158.

827 28. Rodríguez-Comas J, Moreno-Asso A, Moreno-Vedia J, Martín M, Castaño C,
828 Marzà-Florensa A, et al. Stress-Induced MicroRNA-708 Impairs β-Cell Function
829 and Growth. Diabetes. 2017 Dec 1;66(12):3029–40.

830 29. Lin K-T, Yeh Y-M, Chuang C-M, Yang SY, Chang J-W, Sun S-P, et al.
831 Glucocorticoids mediate induction of microRNA-708 to suppress ovarian
832 cancer metastasis through targeting Rap1B. Nat Commun. 2015 Jan
833 8;6(1):5917.

834 30. Behrman S, Acosta-Alvear D, Walter P. A CHOP-regulated microRNA controls
835 rhodopsin expression. J Cell Biol. 2011 Mar 21;192(6):919–27.

836 31. Chen RJ, Kelly G, Sengupta A, Heydendael W, Nicholas B, Beltrami S, et al.
837 MicroRNAs as biomarkers of resilience or vulnerability to stress. Neuroscience.
838 2015 Oct 1;305:36–48.

839 32. Oyang EL, Davidson BC, Lee W, Poon MM. Functional Characterization of the
840 Dendritically Localized mRNA Neuronatin in Hippocampal Neurons. Amédée T,
841 editor. PLoS ONE. 2011 Sep 14;6(9):e24879.

842 33. Vatsa N, Kumar V, Singh BK, Kumar SS, Sharma A, Jana NR. Down-Regulation of
843 miRNA-708 Promotes Aberrant Calcium Signaling by Targeting Neuronatin in a
844 Mouse Model of Angelman Syndrome. Front Mol Neurosci. 2019 Feb 13;12:35.

845 34. Ryu S, McDonnell K, Choi H, Gao D, Hahn M, Joshi N, et al. Suppression of
846 miRNA-708 by Polycomb Group Promotes Metastases by Calcium-Induced Cell
847 Migration. Cancer Cell. 2013 Jan;23(1):63–76.

848 35. Braun JL, Teng ACT, Geromella MS, Ryan CR, Fenech RK, MacPherson REK, et al.
849 Neuronatin promotes SERCA uncoupling and its expression is altered in skeletal
850 muscles of high-fat diet-fed mice. FEBS Lett. 2021;595(22):2756–67.

851 36. Lin H-H, Bell E, Uwanogho D, Perfect LW, Noristani H, Bates TJD, et al. Neuronatin
852 Promotes Neural Lineage in ESCs via Ca2+ Signaling. Stem Cells. 2010 Nov
853 1;28(11):1950–60.

37. Viswanath B, Jose SP, Squassina A, Thirthalli J, Purushottam M, Mukherjee O, et al. Cellular models to study bipolar disorder: A systematic review. J Affect Disord. 2015 Sep 15;184:36–50.

38. Harrison PJ, Hall N, Mould A, Al-Juffali N, Tunbridge EM. Cellular calcium in bipolar disorder: systematic review and meta-analysis. Mol Psychiatry. 2021 Aug;26(8):4106–16.

39. Kircher T, Wöhr M, Nenadic I, Schwarting R, Schratt G, Alferink J, et al. Neurobiology of the major psychoses: a translational perspective on brain structure and function—the FOR2107 consortium. Eur Arch Psychiatry Clin Neurosci. 2019 Dec 1;269(8):949–62.

40. Wittchen H-U, Wunderlich U, Gruschwitz S, Zaudig M. SKID I. Strukturiertes Klinisches Interview für DSM-IV. Achse I: Psychische Störungen. Interviewheft und Beurteilungsheft. Eine deutschsprachige, erweiterte Bearb. d. amerikanischen Originalversion des SKID I. 1997;

41. World Health Organization, editor. The ICD-10 classification of mental and behavioural disorders: clinical descriptions and diagnostic guidelines. Geneva: World Health Organization; 1992. 362 p.

42. Walker EA, Gelfand A, Katon WJ, Koss MP, Von Korff M, Bernstein D, et al. Adult health status of women with histories of childhood abuse and neglect. Am J Med. 1999 Oct 1;107(4):332–9.

43. Brickenkamp R. Der Aufmerksamkeits-Belastungstest d2. Hogrefe, Göttingen; 2002.

44. Chen C-J, Servant N, Toedling J, Sarazin A, Marchais A, Duvernois-Berthet E, et al. ncPRO-seq: a tool for annotation and profiling of ncRNAs in sRNA-seq data. Bioinformatics. 2012 Dec 1;28(23):3147–9.

45. Ritchie ME, Phipson B, Wu D, Hu Y, Law CW, Shi W, et al. limma powers differential expression analyses for RNA-sequencing and microarray studies. Nucleic Acids Res. 2015 Apr 20;43(7):e47.

46. Christensen M. Recombinant adeno-associated virus-mediated microRNA delivery into the postnatal mouse brain reveals a role for miR-134 in dendritogenesis in vivo. Front Neural Circuits. 2010;

47. Daswani R, Gilardi C, Soutschek M, Nanda P, Weiss K, Bicker S, et al. MicroRNA-138 controls hippocampal interneuron function and short-term memory in mice. Huguenard JR, editor. eLife. 2022 Mar 15;11:e74056.

48. Levone BR, Moloney GM, Cryan JF, O'Leary OF. Specific sub-regions along the longitudinal axis of the hippocampus mediate antidepressant-like behavioral effects. Neurobiol Stress. 2021 May;14:100331.

49. Can A, Dao DT, Terrillion CE, Piantadosi SC, Bhat S, Gould TD. The Tail Suspension Test. J Vis Exp JoVE. 2012 Jan 28;(59):3769.

50. Dobin A, Davis CA, Schlesinger F, Drenkow J, Zaleski C, Jha S, et al. STAR: ultrafast universal RNA-seq aligner. Bioinformatics. 2013 Jan 1;29(1):15–21.

51. Liao Y, Smyth GK, Shi W. featureCounts: an efficient general purpose program for assigning sequence reads to genomic features. Bioinformatics. 2014 Apr 1;30(7):923–30.

52. Robinson MD, McCarthy DJ, Smyth GK. edgeR: a Bioconductor package for differential expression analysis of digital gene expression data. Bioinformatics. 2010 Jan 1;26(1):139–40.

53. Leek JT, Johnson WE, Parker HS, Jaffe AE, Storey JD. The sva package for removing batch effects and other unwanted variation in high-throughput experiments. Bioinformatics. 2012 Mar 15;28(6):882–3.

54. Agarwal V, Bell GW, Nam J-W, Bartel DP. Predicting effective microRNA target sites in mammalian mRNAs. Izaurralde E, editor. eLife. 2015 Aug 12;4:e05005.

55. Craddock N, O'Donovan MC, Owen MJ. The genetics of schizophrenia and bipolar disorder: dissecting psychosis. J Med Genet. 2005 Mar 1;42(3):193–204.

56. Vieta E, Salagre E, Grande I, Carvalho AF, Fernandes BS, Berk M, et al. Early Intervention in Bipolar Disorder. Am J Psychiatry. 2018 May;175(5):411–26.

57. Nierenberg AA, Agustini B, Köhler-Forsberg O, Cusin C, Katz D, Sylvia LG, et al. Diagnosis and Treatment of Bipolar Disorder: A Review. JAMA. 2023 Oct 10;330(14):1370.

58. Cao R, López-de-Ullibarri I. ROC Curves for the Statistical Analysis of Microarray Data. In: Bolón-Canedo V, Alonso-Betanzos A, editors. Microarray Bioinformatics. New York, NY: Springer New York; 2019. p. 245–53. (Methods in Molecular Biology; vol. 1986).

59. Yao Z, van Velthoven CTJ, Nguyen TN, Goldy J, Sedeno-Cortes AE, Baftizadeh F, et al. A taxonomy of transcriptomic cell types across the isocortex and hippocampal formation. Cell. 2021 Jun;184(12):3222-3241.e26.

60. Bhat S, Dao DT, Terrillion CE, Arad M, Smith RJ, Soldatov NM, et al. CACNA1C (Cav1.2) in the pathophysiology of psychiatric disease. Prog Neurobiol. 2012 Oct 1;99(1):1–14.

61. Harrison PJ, Husain SM, Lee H, Los Angeles AD, Colbourne L, Mould A, et al. CACNA1C (CaV1.2) and other L-type calcium channels in the pathophysiology and treatment of psychiatric disorders: Advances from functional genomics and pharmacoepidemiology. Neuropharmacology. 2022 Dec 1;220:109262.

62. Ferreira MAR, O'Donovan MC, Meng YA, Jones IR, Ruderfer DM, Jones L, et al. Collaborative genome-wide association analysis supports a role for ANK3 and CACNA1C in bipolar disorder. Nat Genet. 2008 Sep;40(9):1056–8.

931 63. Dedic N, Pöhlmann ML, Richter JS, Mehta D, Czamara D, Metzger MW, et al.
932 Cross-disorder risk gene CACNA1C differentially modulates susceptibility to
933 psychiatric disorders during development and adulthood. Mol Psychiatry.
934 2018;23(3):533–43.

935 64. Dao DT, Mahon PB, Cai X, Kovacsics CE, Blackwell RA, Arad M, et al. Mood
936 Disorder Susceptibility Gene CACNA1C Modifies Mood-Related Behaviors in
937 Mice and Interacts with Sex to Influence Behavior in Mice and Diagnosis in
938 Humans. Biol Psychiatry. 2010 Nov;68(9):801–10.

939 65. Bavley CC, Fischer DK, Rizzo BK, Rajadhyaksha AM. Cav1.2 channels mediate
940 persistent chronic stress-induced behavioral deficits that are associated with
941 prefrontal cortex activation of the p25/Cdk5-glucocorticoid receptor pathway.
942 Neurobiol Stress. 2017 Dec 1;7:27–37.

943 66. Seffer D, Rippberger H, Schwarting RKW, Wöhr M. Pro-social 50-kHz ultrasonic
944 communication in rats: post-weaning but not post-adolescent social isolation
945 leads to social impairments—phenotypic rescue by re-socialization. Front Behav
946 Neurosci. 2015 May 1;9.

947 67. Namkung H, Yukitake H, Fukudome D, Lee BJ, Tian M, Ursini G, et al. The miR-
948 124-AMPAR pathway connects polygenic risks with behavioral changes shared
949 between schizophrenia and bipolar disorder. Neuron. 2023 Jan 18;111(2):220-
950 235.e9.

951 68. Huang Y, Zhang Z, Lin S, Zhou H, Xu G. Cognitive Impairment Mechanism in
952 Patients with Bipolar Disorder. Neuropsychiatr Dis Treat. 2023 Feb;Volume
953 19:361–6.

954 69. Camelo EVM, Mograbi D, de Assis da Silva R, Bifano J, Wainstok M, Silveira LAS,
955 et al. Performance of Bipolar Disorder Patients in Attention Testing: Comparison
956 with Normal Controls and Among Manic, Depressive, and Euthymic Phases.
957 Psychiatr Q. 2017 Mar 1;88(1):55–63.

958 70. Fee C, Banasr M, Sibille E. Somatostatin-Positive Gamma-Aminobutyric Acid
959 Interneuron Deficits in Depression: Cortical Microcircuit and Therapeutic
960 Perspectives. Biol Psychiatry. 2017 Oct;82(8):549–59.

961 71. Lewis DA, Sweet RA. Schizophrenia from a neural circuitry perspective:
962 advancing toward rational pharmacological therapies. J Clin Invest. 2009 Apr
963 1;119(4):706–16.

964 72. Sakai T, Oshima A, Nozaki Y, Ida I, Haga C, Akiyama H, et al. Changes in density
965 of calcium-binding-protein-immunoreactive GABAergic neurons in prefrontal
966 cortex in schizophrenia and bipolar disorder. Neuropathology. 2008;28(2):143–
967 50.

968 73. Fung SJ, Fillman SG, Webster MJ, Shannon Weickert C. Schizophrenia and
969 bipolar disorder show both common and distinct changes in cortical
970 interneuron markers. Schizophr Res. 2014 May 1;155(1):26–30.

74. Sharma J, Mukherjee D, Rao SNR, Iyengar S, Shankar SK, Satishchandra P, et al. Neuronatin-mediated Aberrant Calcium Signaling and Endoplasmic Reticulum Stress Underlie Neuropathology in Lafora Disease. J Biol Chem. 2013 Mar;288(13):9482–90.

75. Burmeister M, McInnis MG, Zöllner S. Psychiatric genetics: progress amid controversy. Nat Rev Genet. 2008 Jul;9(7):527–40.

76. Craddock N, Sklar P. Genetics of bipolar disorder: successful start to a long journey. Trends Genet. 2009 Feb;25(2):99–105.

77. Robinson N, Bergen SE. Environmental Risk Factors for Schizophrenia and Bipolar Disorder and Their Relationship to Genetic Risk: Current Knowledge and Future Directions. Front Genet. 2021;12.

78. Toda T, Parylak S, Linker SB, Gage FH. The role of adult hippocampal neurogenesis in brain health and disease. Mol Psychiatry. 2019 Jan;24(1):67–87.

79. Wöhr M, Kisko TM, Schwarting RKW. Social Behavior and Ultrasonic Vocalizations in a Genetic Rat Model Haploinsufficient for the Cross-Disorder Risk Gene Cacna1c. Brain Sci. 2021 Jun;11(6):724.

80. Srinivasan S, Shariff M, Bartlett S. The Role of the Glucocorticoids in Developing Resilience to Stress and Addiction. Front Psychiatry. 2013;4.

81. Hewitt T, Alural B, Tilak M, Wang J, Becke N, Chartley E, et al. Bipolar disorder-iPSC derived neural progenitor cells exhibit dysregulation of store-operated Ca2+ entry and accelerated differentiation. Mol Psychiatry. 2023 Jul 4;1–14.

82. Zou H-Y, Guo L, Zhang B, Chen S, Wu X-R, Liu X-D, et al. Aberrant miR-339-5p/neuronatin signaling causes prodromal neuronal calcium dyshomeostasis in mutant presenilin mice. J Clin Invest. 2022 Apr 15;132(8):e149160.

83. Wang Q-C, Zheng Q, Tan H, Zhang B, Li X, Yang Y, et al. TMCO1 Is an ER Ca 2+ Load-Activated Ca 2+ Channel. Cell. 2016 Jun;165(6):1454–66.

84. Daverkausen-Fischer L, Pröls F. Regulation of calcium homeostasis and flux between the endoplasmic reticulum and the cytosol. J Biol Chem. 2022 Jul 1;298(7):102061.

85. Tu H, Nelson O, Bezprozvanny A, Wang Z, Lee S-F, Hao Y-H, et al. Presenilins Form ER Ca2+ Leak Channels, a Function Disrupted by Familial Alzheimer's Disease-Linked Mutations. Cell. 2006 Sep 8;126(5):981–93.

86. Bezprozvanny I, Mattson MP. Neuronal calcium mishandling and the pathogenesis of Alzheimer's disease. Trends Neurosci. 2008 Sep 1;31(9):454–63.

87. Banach E, Dmitrzak-Weglarz M, Pawlak J, Kapelski P, Szczepankiewicz A, Rajewska-Rager A, et al. Dysregulation of miR-499, miR-708 and miR-1908

during a depression episode in bipolar disorders. Neurosci Lett. 2017 Jul;654:117–9.

88. Diflorio A, Jones I. Is sex important? Gender differences in bipolar disorder. Int Rev Psychiatry. 2010 Oct 1;22(5):437–52.

89. Arnold LM, McElroy SL, Keck PE. The role of gender in mixed mania. Compr Psychiatry. 2000;41(2):83–7.

90. Slyepchenko A, Frey BN, Lafer B, Nierenberg AA, Sachs GS, Dias RS. Increased illness burden in women with comorbid bipolar and premenstrual dysphoric disorder: data from 1 099 women from STEP-BD study. Acta Psychiatr Scand. 2017 Nov;136(5):473–82.

91. Tondo L, Baldessarini RJ. Rapid cycling in women and men with bipolar manic-depressive disorders. Am J Psychiatry. 1998 Oct;155(10):1434–6.

92. Clements C, Morriss R, Jones S, Peters S, Roberts C, Kapur N. Suicide in bipolar disorder in a national English sample, 1996-2009: frequency, trends and characteristics. Psychol Med. 2013 Dec;43(12):2593–602.

93. Lobentanzer S, Hanin G, Klein J, Soreq H. Integrative Transcriptomics Reveals Sexually Dimorphic Control of the Cholinergic/Neurokine Interface in Schizophrenia and Bipolar Disorder. Cell Rep. 2019 Oct 15;29(3):764-777.e5.

1038

1039 # Figure legends

1040

1041 **Fig. 1 miR-708-5p is upregulated in the peripheral blood of human subjects at**
1042 **risk for or diagnosed with MDs**.

1043

1044 **A.** Schematic representation of the workflow to obtain PBMCs samples from the
1045 FOR2107 cohort (see also materials and methods) (39). Subjects underwent
1046 psychiatric and cognitive evaluation. After the data was collected, blood was
1047 withdrawn and PBMCs prepared followed by RNA extraction and downstream
1048 gene expression analysis. Samples were collected from psychiatrically healthy
1049 female subjects (CTL), or psychiatrically healthy female subjects with genetic
1050 predisposition for mood disorder (GR) or that suffered from childhood
1051 maltreatment (ER) (Vulnerability samples). Samples were also collected from
1052 male and female patients that were diagnosed with Major Depressive Disorder
1053 (MDD) or Bipolar Disorder (BD) (mood disorder samples).

1054 **B. and C.** Volcano plot depicting miRNAs differentially expressed based on small
1055 RNA sequencing performed with RNA isolated from PBMCs of control subjects
1056 (CTL; n=18), healthy subjects who suffered childhood maltreatment
1057 (Environmental risk, ER; n=18), or healthy subjects with a genetic risk (GR;
1058 n=14). CTL vs ER (B) or GR (C): miRNAs that are significantly downregulated
1059 (logFC<0.5, p-value<0.05) are marked in red; miRNAs that are significantly
1060 upregulated (logFC>0.5, p-value<0.05) in blue. Each Volcano Plot is
1061 accompanied by a table showing the top 15 differentially expressed genes
1062 ordered from smallest to largest p-value. miRNAs overlapping between (B)
1063 and (C) are highlighted.

1064 **D.** miR-708-5p qPCR analysis of total RNA isolated from PBMCs of control
1065 subjects (CTL=18), or healthy subjects who suffered childhood Maltreatment
1066 (Environmental risk, ER= 16), or healthy subjects with a genetic risk (GR=18).
1067 One-way ANOVA with Holm-Sidak's multiple comparisons test, HC vs ER, **,
1068 P=0.0064; HC vs GR, ***, P=0.0006; ER vs GR, ns. Data are presented as violin
1069 plots with median, quartiles and data points.

1070 **E.** miR-708-5p qPCR analysis of total RNA isolated from PBMCs of female
1071 patients diagnosed with BD or MDD (control: CTL= 26; MDD= 18; BD= 26).
1072 Wilcoxon rank-sum test after correction for age and antidepressant treatment;
1073 linear model of the form -DeltaCq ~ Group + Age + Antidepressant treatment.
1074 Females: CTL vs MDD, *, p<0.05; CTL vs BD, ****, p<0.0005.

1075 **F.** miR-708-5p qPCR analysis of total RNA isolated from PBMCs of male patients
1076 diagnosed with BD or MDD (control: CTL=31; MDD=24; BD= 37. Wilcoxon
1077 rank-sum test after correction for age and antidepressant treatment; linear
1078 model of the form -DeltaCq ~ Group + Age + Antidepressant treatment. CTL
1079 vs MDD, p=0.0549; CTL vs BD, ****, p<0.0005). Data are presented as violin
1080 plots with median, quartiles and data points.

1081 **G.** Correlation plot between the peripheral levels of miR-708-5p in male BD
1082 samples (n=37) and Young Mania Rating Scale. Spearman correlation
1083 coefficient with two-tailed analysis. Data are presented as XY tables.

1084 **H.** Correlation plot between the peripheral levels of miR-708-5p in female
1085 samples (n=26) and Young Mania Rating Scale. Spearman correlation
1086 coefficient with two-tailed analysis. Data are presented as XY tables.

1087 **I.** ROC curve of combined miR-708-5p and miR-499-5p expression in female
1088 (left) and male (right) subjects to discriminate BD vs controls and MDD
1089 samples. The indicated thresholds are the closest point to the optimal (i.e. top-
1090 left).

1091

1092 **Figure 2. miR-708-5p is expressed in rat hippocampal neurons and upregulated**
1093 **in the hippocampus of rat models of environmental or genetic risk for MDs.**

1094

1095 **A.** miR-708-5p qPCR analysis using total RNA isolated from different areas of the
1096 adult female rat brain. Data are represented as bar graphs, mean ± SD (n=3
1097 animals).

1098 **B.** Single-molecule fluorescence *in situ* hybridization (smFISH) performed in rat
1099 hippocampal neurons at 7 days *in vitro* (DIV7) using probes directed against miR-
1100 708-5p (red channel) and CamK2a (green channel) to identify excitatory neurons.
1101 Scale bar: 20μm.

1102 **C.** smFISH performed in rat hippocampal neurons at DIV7 using probes against
1103 miR-708-5p (red channel) and Gad2 (green channel) to identify inhibitory
1104 neurons. Scale bar: 20μm.

1105 **D.** Relative expression of miR-708-5p in primary rat hippocampal neurons at
1106 different DIV (n = 3 independent experiments) normalized to U6 snRNA. Data are
1107 represented on XY graph as mean ±SD.

1108 **E.** Schematic representation of the juvenile social isolation experiment, n=9 for
1109 each experimental group; PND: postnatal day.

1110 **F.** miR-708-5p qPCR analysis of total RNA isolated from hippocampi of Wild type
1111 (WT) or *Cacna1c*$^{+/-}$ male juvenile rats that were either group-housed or socially
1112 isolated for four weeks (n=9 in each group). WT group-housed vs WT Isolated: *,
1113 p=0.0265; WT group-housed vs *Cacna1c*$^{+/-}$: **, p=0.0026; linear mixed model, -
1114 DeltaCq ~ Genotype * Housing + (1| Cohort), followed by post hoc pairwise
1115 comparison with emmeans package (pairwise ~ Genotype * Housing); ns: non-
1116 significant. Data are represented as box plot with whiskers and data points (+:
1117 mean, line: median; whiskers: minimum and maximum values).

1118

1119 **Figure 3. miR-708-5p overexpression in the mouse hippocampus recapitulates**
1120 **BD-associated endophenotypes.**

1121

1122 **A.** Schematic timeline of the acute rAAV stereotactic injection of control (hpCTL) or
1123 miR-708-OE (hp708) virus into the dorsal and ventral hippocampus of mice at
1124 PNW 7/8, followed by behavioral testing at PNW 11/12.

1125 **B.** Coronal brain section of mouse brains displaying intense GFP expression upon
1126 infection with hp708 virus in the dorsal (up) and ventral (down) hippocampus.
1127 Scale bar: 2000 µm.

1128 **C.** miR-708-5p qPCR analysis of total RNA isolated from hippocampus of mice that
1129 underwent behavioral testing. upon miR-708-5p overexpression. hpCTL n=39,
1130 hp708 n=39. Unpaired t-Test, ****, p<0.00001. Data are represented as box plot
1131 with whiskers and data points (+: mean, line: median; whiskers: minimum and
1132 maximum values).

1133 **D.** Tail Suspension Test. Time (s) male mice injected with the indicated rAAV (hpCTL
1134 or hp708, n=15 each) spent immobile. Data are represented as box plot with
1135 whiskers and data points (+: mean, line: median; whiskers: minimum and
1136 maximum values). Unpaired t-test, ****, p<0.0001.

1137 **E.** Tail Suspension Test. Time (s) female mice injected with the indicated rAAV
1138 (hpCTL n= 12, or hp708, n=11) spent immobile. Data are represented as box plot
1139 with whiskers and data points (+: mean, line: median; whiskers: minimum and
1140 maximum values). Unpaired t-test, ns.

1141 **F.** Marble Burying test. Number of marbles male mice injected with the indicated
1142 rAAV (hpCTL n= 11, or hp708, n=12) buried in 30 minutes. Data are represented
1143 as box plot with whiskers and data points (+: mean, line: median; whiskers:
1144 minimum and maximum values). Unpaired t-test, ns, p=0.0524.

1145 **G.** Schematic representation of the Novel Object Recognition (NOR) Test.mice are
1146 exposed to two familiar objects during the familiarization phase. After five

minutes, they are returned to the home cage for either 24 hours or 5 minutes. They are then exposed to a novel and a familiar object during the test phase.

H. Novel object recognition Test with 24 hours break in between familiarization and novelty testing. Time (s) male mice injected with the indicated rAAV (hpCTL n= 10, or hp708, n=12) explored either the familiar (F) or novel (N) object. Data are represented as box plot with whiskers and data points (+: mean, line: median; whiskers: minimum and maximum values). Two-way RM ANOVA: Novelty x Group, ***, p=0.0004; Novelty, ****, p<0.0001; Group, ns, p=0.8830. Šídák's post hoc test, F vs N: hpCTL, ****, p<0.0001; hp708, ns, p=0.6735.

I. Novel object recognition Test with 5 minutes break in between familiarization and novelty testing. Time (s) male mice injected with the indicated rAAV (hpCTL or hp708, n=15 each) explored either the familiar (F) or novel (N) object. Data are represented as box plot with whiskers and data points (+: mean, line: median; whiskers: minimum and maximum values). Two-way RM ANOVA: Novelty x Group, ****, p<0.0001; Novelty, ****, p<0.0001; Group, ns, p=0.8207. Šídák's post hoc test, F vs N: hpCTL, ****, p<0.0001; hp708, ns, p=0.6975.

J. Novel object recognition Test with 5 minutes break in between familiarization and novelty testing. Time (s) female mice injected with the indicated rAAV (hpCTL n= 12, or hp708, n=11) explored either the familiar (F) or novel (N) object. Data are represented as box plot with whiskers and data points (+: mean, line: median; whiskers: minimum and maximum values). Two-way RM ANOVA: Novelty x Group, *, p<0.0130; Novelty, ***, p=0.0001; Group, ns, p=0.8143. Šídák's post hoc test, F vs N: hpCTL, ****, p<0.0001; hp708, ns, p=0.3127.

K. Pearson correlation plot of miR708 peripheral levels and attention (d2 test) in all human participants (female + male, CTL + MDD + BD, n=162), **, p=.005, r=-.223.

Figure 4. miR-708-5p directly targets Nnat, an ER-resident protein involved in calcium homeostasis.

A. Volcano plot depicting differential gene expression in the hippocampus between hp708 and hpCTL injected mice based on polyA-RNA sequencing.

B. Heatmap displaying miR-708-5p predicted targets which are significantly downregulated from (A), as well as their expression in different cell types based on single-cell RNA-seq data (Allen 10X+smartSeq taxonomy)(59). The red rectangle highlights Nnat.

1183 **C.** Nucleotide base pairing depicting the perfect binding of miR-708-5p with the
1184 mouse Nnat 3'-UTR.

1185 **D.** miR-708-5p qPCR analysis of total RNA isolated from mouse hippocampi upon
1186 miR-708-5p overexpression. hpCTL n=17, hp708 n=17. Unpaired t-Test, ****,
1187 p<0.00001. Data are represented as box plot with whiskers and data points (+:
1188 mean, line: median; whiskers: minimum and maximum values).

1189 **E.** Neuronatin qPCR analysis of total RNA isolated from mouse hippocampi upon
1190 miR-708-5p overexpression. hpCTL n=13, hp708 n=15. Unpaired t-Test, ****,
1191 p=0.0269. Data are represented as box plot with whiskers and data points (+:
1192 mean, line: median; whiskers: minimum and maximum values).

1193 **F.** miR-708-5p qPCR analysis of total RNA isolated from rat primary hippocampal
1194 neurons at DIV20 infected with hpCTL or hp708 for miR-708-5p overexpression.
1195 hpCTL n=4, hp708 n=5. Unpaired t-Test, *, p=0.0317. Data are represented as
1196 box plot with whiskers and data points (+: mean, line: median; whiskers:
1197 minimum and maximum values).

1198 **G.** Neuronatin qPCR analysis of total RNA isolated from rat primary hippocampal
1199 neurons at DIV20 infected with hpCTL or hp708 for miR-708-5p overexpression.
1200 hpCTL n=4, hp708 n=5. Unpaired t-Test, *, p=0.0159. Data are represented as
1201 box plot with whiskers and data points (+: mean, line: median; whiskers:
1202 minimum and maximum values).

1203 **H.** Representative Western blot image of Nnat (lower panel) and Tubulin (upper
1204 panel) protein expression levels in hippocampal neurons (DIV20) that were
1205 infected with hpCTL or hp708 for miR-708-5p overexpression on DIV2. Tubulin
1206 was used as a loading control.

1207 **I.** Quantification of the relative intensity of Nnat protein levels in hippocampal
1208 neurons (DIV20) that were infected with hpCTL or hp708 for miR-708-5p
1209 overexpression on DIV2 based on (G). Tubulin was used as normalizer. Ratio-
1210 paired t-test, **, p=0.0042. n=4 per experimental group. Data are represented as
1211 box plot with whiskers and data points (+: mean, line: median; whiskers:
1212 minimum and maximum values).

1213 **J.** Relative luciferase activity of rat hippocampal neurons transfected with the
1214 indicated plasmid (Control: hpCTL-p; overexpressing miR-708-5p: hp708-p) and
1215 expressing either Nnat wild-type (wt) or miR-708-5p binding site mutant (mt)
1216 reporter genes. Data are represented as scattered dot plots with bar, mean±SD
1217 (n=4 independent experiments; Two-way ANOVA: main effect of the hairpin
1218 *p=0.0245, of the Nnat luciferase reporter **p=0.0050, and of the hairpin by
1219 Nnat luciferase reporter interaction p<0.0374. Sidak's post hoc test: **p=0.0092).

1220 **K.** Relative luciferase activity of rat hippocampal neurons transfected with the
1221 indicated plasmid (Control: spCTL-p; knocking-down miR-708-5p: sp708-p) and
1222 expressing either Nnat wt or mt reporter genes. Data are represented as
1223 scattered dot plots with bar, mean±SD (n=4 independent experiments; Two-way
1224 ANOVA: main effect of the hairpin *p=0.0211, no main effect of the Nnat
1225 luciferase reporter, or of the hairpin by Nnat luciferase reporter interaction.
1226 Sidak's post hoc test: *p=0.0287).

1227

1228 **Figure 5. Restoring Nnat expression in miR-708-5p overexpressing**
1229 **hippocampal neurons rescues BD-associated behaviors in mice.**

1230

1231 **A.** Schematic representation of the three rAAV constructs used in the rescue
1232 experiment.

1233 **B.** miR-708-5p qPCR analysis of total RNA isolated from the hippocampus of male
1234 mice injected with mCherry-P2A-hpCTL (n=9), mCherry-P2A-hp708 (n12), or
1235 Nnat-P2A-hp708 (n=12) viruses. One-way ANOVA, Post hoc Tukey's Test:
1236 mCherry-P2A-hpCTL vs mCherry-P2A-hp708: ****, p<0.0001, mCherry-P2A-
1237 hpCTL vs Nnat-P2A-hp708: ***, p<0.0001, mCherry-P2A-hp708 vs Nnat-P2A-
1238 hp708: ns, p=0.1225. Data are represented as box plot with whiskers and data
1239 points (+: mean, line: median; whiskers: minimum and maximum values).

1240 **C.** Neuronatin qPCR analysis of total RNA isolated from the hippocampus of male
1241 mice injected with mCherry-P2A-hpCTL (n=9), mCherry-P2A-hp708 (n12), or
1242 Nnat-P2A-hp708 (n=12) viruses. One-way ANOVA, Post hoc Tukey's Test:
1243 mCherry-P2A-hpCTL vs mCherry-P2A-hp708: ***, p=0.0003, mCherry-P2A-
1244 hpCTL vs Nnat-P2A-hp708: ns, p=0.7379, mCherry-P2A-hp708 vs Nnat-P2A-
1245 hp708: ****, p<0.0001. Data are represented as box plot with whiskers and data
1246 points (+: mean, line: median; whiskers: minimum and maximum values).

1247 **D.** Novel object recognition Test with 5 minutes break in between familiarization and
1248 novelty testing. Time (s) male mice injected with the indicated rAAV (mCherry-
1249 P2A-hpCTL (n=9), mCherry-P2A-hp708 (n12), or Nnat-P2A-hp708 (n=12))
1250 explored either the familiar (F) or novel (N) object. Data are represented as box
1251 plot with whiskers and data points (+: mean, line: median; whiskers: minimum
1252 and maximum values). Two-way RM ANOVA: Novelty x Group, ****, p<0.0001;
1253 Novelty, ****, p<0.0001; Group, ns, p=0.5765. Šídák's post hoc test, F vs N:
1254 mCherry-P2A-hpCTL, ****, p<0.0001; mCherry-P2A-hp708, ns, p=0.6534; Nnat-
1255 P2A-hp708, ****, p<0.0001.

1256 **E.** Tail Suspension Test. Time (s) male mice injected with the indicated rAAV
1257 (mCherry-P2A-hpCTL (n=9), mCherry-P2A-hp708 (n12), or Nnat-P2A-hp708

1258 (n=12)) spent immobile. One-way ANOVA, Post hoc Tukey's Test: mCherry-P2A-
1259 hpCTL vs mCherry-P2A-hp708: ****, p<0.0001, mCherry-P2A-hpCTL vs Nnat-
1260 P2A-hp708: ns, p=0.9617, mCherry-P2A-hp708 vs Nnat-P2A-hp708: ****,
1261 p<0.0001. Data are represented as box plot with whiskers and data points (+:
1262 mean, line: median; whiskers: minimum and maximum values).

1263

1264

1265 **Table 1.**

	Control	**BD**	**MDD**	**P Value**
n (f/m)	26/31	26/37	18/24	N/A
Age ± *S.D.*	29.4 ± 5.4/ 39.7± 13.4	29.9 ± 5.4/ 41.7 ± 11.3	29.6± 4.9/ 39.3.6± 14.7	0.94/0.75
CTQ ± *S.D.* (%)	40.7 ± 11.4 (53.8%)	42.3 ± 13.2 (30.8%)	50.2 ± 20.2 (61%)	0.1067/0.4170
Family history of MDs (%)	8 (30.8%)/ 5 (16.1%)	10 (38.5%)/ 10 (27.0%)	5 (27.8%)/ 7 (29.1%)	N/A
HAMD ± *S.D.*	2.7 ± 3.9/ 1.5 ± 2.5	7.5 ± 6.2/ 8.6 ± 6.4	14.8 ± 6.7/ 10.3 ± 7.7	<0.0001
YMRS ± *S.D.*	0.5 ± 1.1/ 0.7 ± 1.7	2.4 ± 2.9/ 7.0 ± 8.2	1.4 ± 1.6/ 1.7 ± 2.2	<0.01/ <0.0001
BDI ± *S.D.*	6.1 ± 6.1/ 4.5 ± 3.9	12.9 ± 11.1/ 12.9 ±9.6	26.6 ± 11.0/ 16.6 ± 10.7	<0.0001
AD (%)	0 (0%)	7 (26.9%)/ 17 (45.95%)	16 (88.9%)/ 17 (70.83%)	N/A
Antipsychotic (%)	0 (0%)	12 (46.15%)/ 19 (51.35%)	7 (38.89%)/ 4 (16.67%)	N/A
Lithium (%)	0 (0%)	4 (15.38%)/ 12 (32.43%)	1 (5.56%)/ 0 (0%)	N/A
Anticonvulsive (%)	0 (0%)	6 (23.08%)/ 10 (27.03%)	1 (5.56%)/ 1 (4.17%)	N/A
Stimulants (%)	0 (0%)	0 (0%)/ 1 (2.70%)	0 (0%)/ 2 (8.33%)	N/A

Benzodiazepine (%)	0 (0%)	0 (0%)	1 (5.56%)/ 0 (0%)	N/A
Z substance (%)	0 (0%)	0 (0%)/ 1 (2.70%)	1 (5.56%)	N/A

Subjects for miR-708-5p expression analysis on psychiatrically healthy controls (Control), Bipolar disorder patients (BD) or Major Depressive Disorder patients (MDD). One-way-ANOVA was performed to evaluate significant differences between groups. S.D.: standard deviation, CTQ: Childhood Maltreatment Questionnaire, HAMD: Hamilton Depression Rating Scale, YMRS: Young Mania Rating Scale, BDI: Beck's Depression Inventory, AD: antidepressant use.

Figures

Fig. 1 miR-708-5p is upregulated in the peripheral blood of human subjects at risk for or diagnosed with MDs.

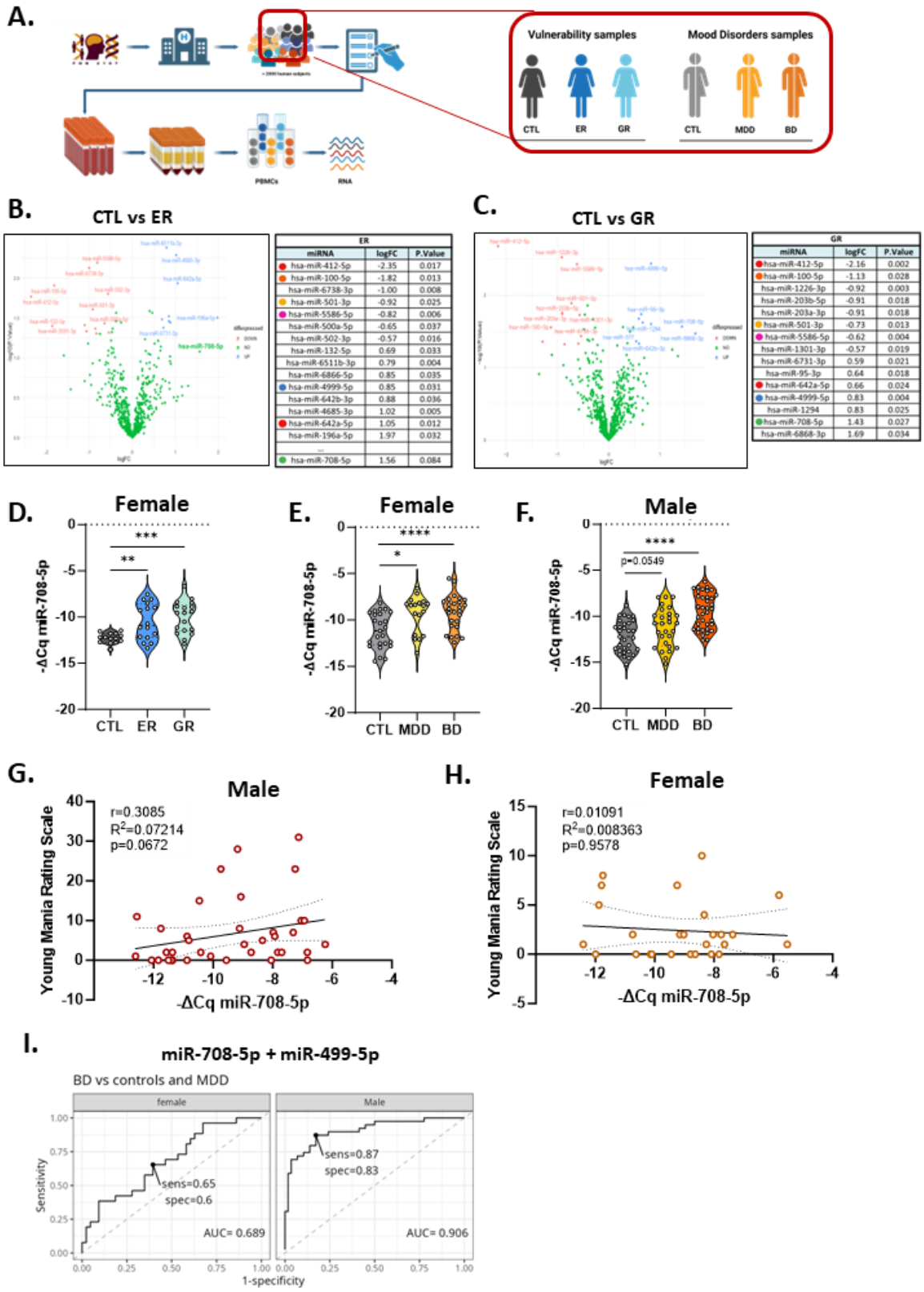

ER		
miRNA	logFC	P.Value
hsa-miR-412-5p	-2.35	0.017
hsa-miR-100-5p	-1.82	0.013
hsa-miR-6738-3p	-1.00	0.008
hsa-miR-501-3p	-0.92	0.025
hsa-miR-5586-5p	-0.82	0.006
hsa-miR-500a-5p	-0.65	0.037
hsa-miR-502-3p	-0.57	0.016
hsa-miR-132-5p	0.69	0.033
hsa-miR-6511b-3p	0.79	0.004
hsa-miR-6866-5p	0.85	0.035
hsa-miR-4999-5p	0.85	0.031
hsa-miR-642b-3p	0.88	0.036
hsa-miR-4685-3p	1.02	0.005
hsa-miR-642a-5p	1.05	0.012
hsa-miR-196a-5p	1.97	0.032
...		
hsa-miR-708-5p	1.56	0.084

GR		
miRNA	logFC	P.Value
hsa-miR-412-5p	-2.16	0.002
hsa-miR-100-5p	-1.13	0.028
hsa-miR-1226-3p	-0.92	0.003
hsa-miR-203b-5p	-0.91	0.018
hsa-miR-203a-3p	-0.91	0.018
hsa-miR-501-3p	-0.73	0.013
hsa-miR-5586-5p	-0.62	0.004
hsa-miR-1301-3p	-0.57	0.019
hsa-miR-6731-3p	0.59	0.021
hsa-miR-95-3p	0.64	0.018
hsa-miR-642a-5p	0.66	0.024
hsa-miR-4999-5p	0.83	0.004
hsa-miR-1294	0.83	0.025
hsa-miR-708-5p	1.43	0.027
hsa-miR-6868-3p	1.69	0.034

1275 **Figure 2. miR-708-5p is expressed in rat hippocampal neurons and upregulated**
1276 **in the hippocampus of rat models of environmental or genetic risk for MDs.**

1277

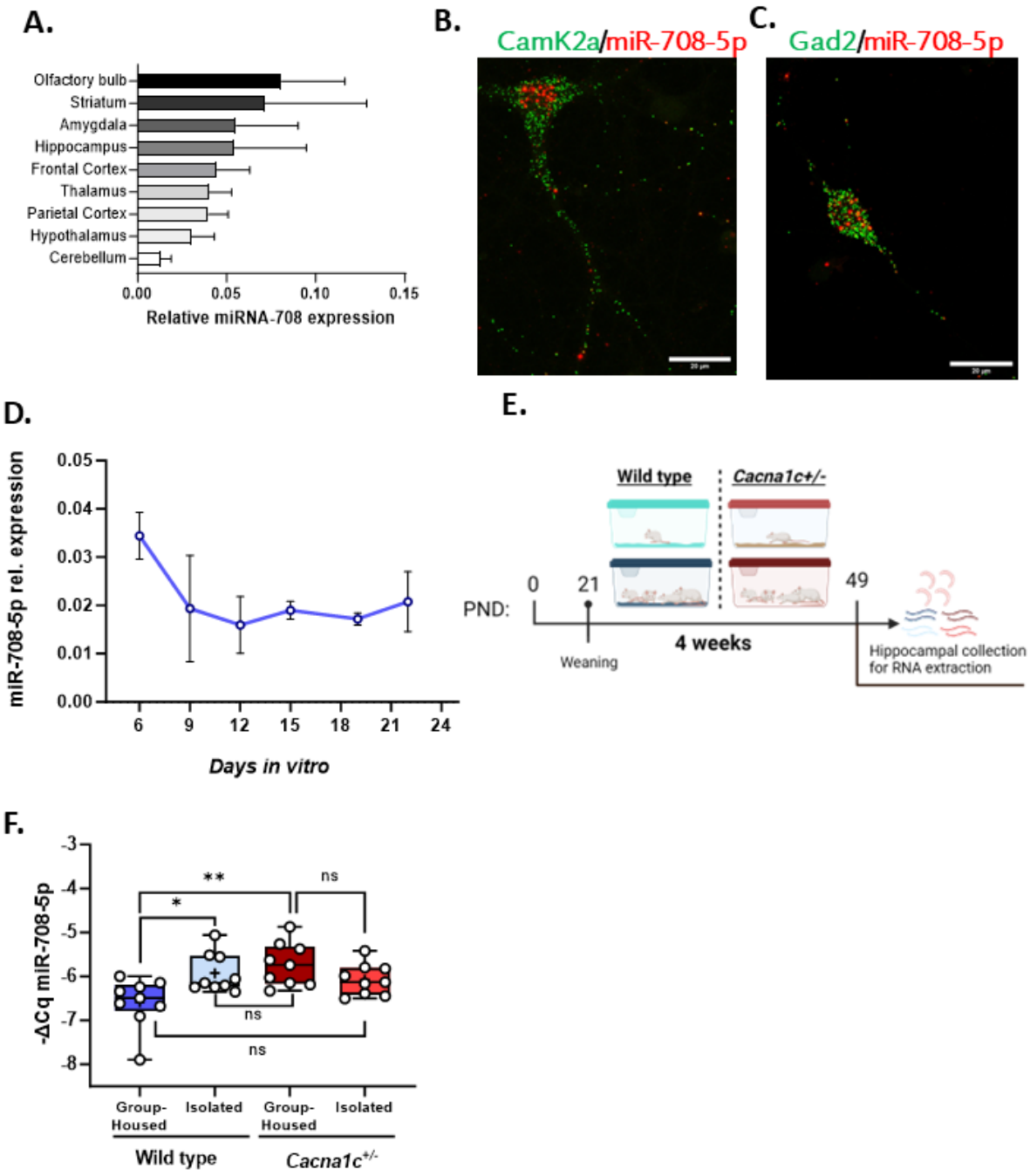

1278 **Figure 3. miR-708-5p overexpression in the mouse hippocampus recapitulates**
1279 **BD-associated endophenotypes.**

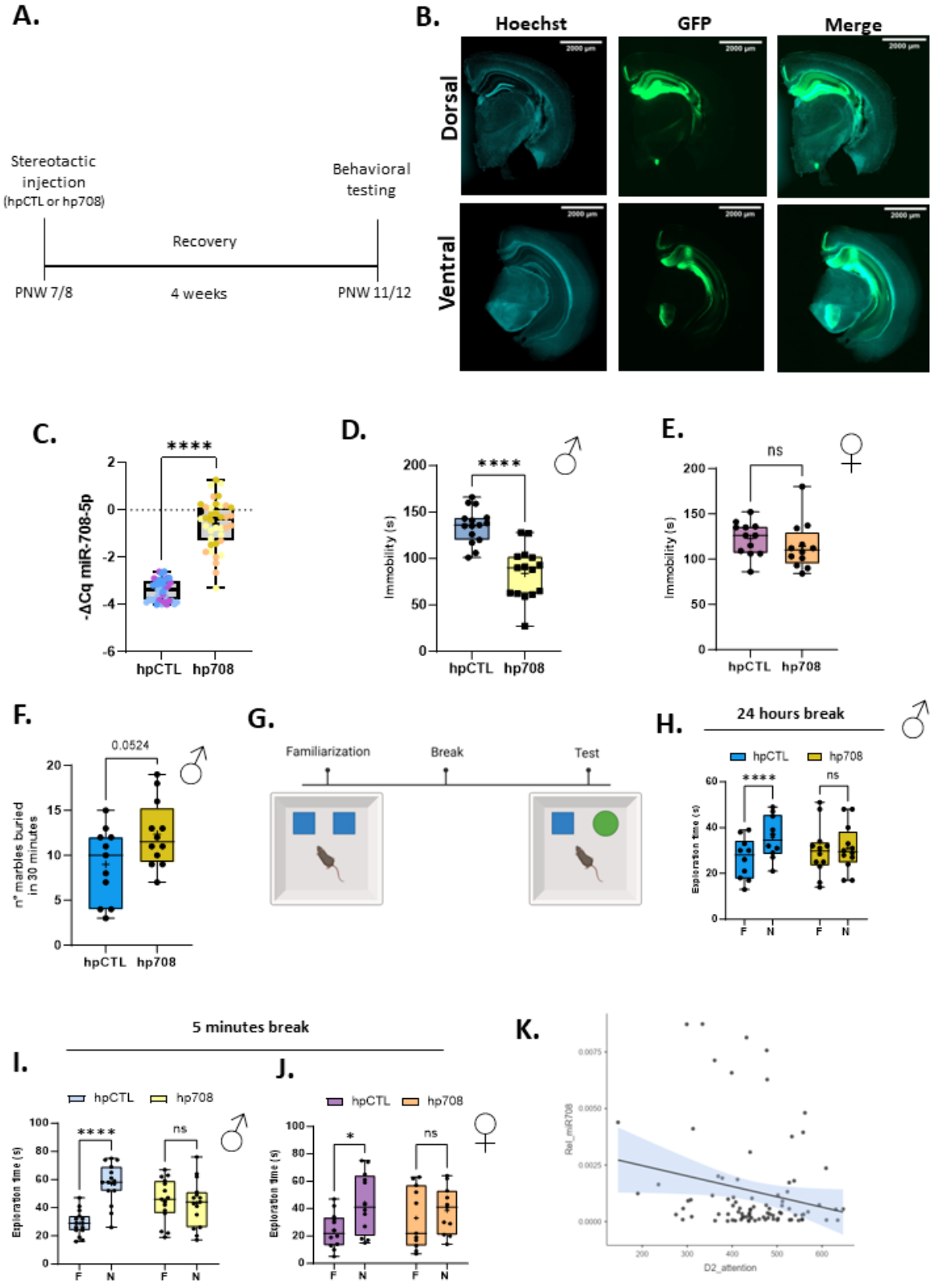

1280 **Figure 4. miR-708-5p directly targets Neuronatin (Nnat), an ER-resident protein**
1281 **involved in calcium homeostasis.**

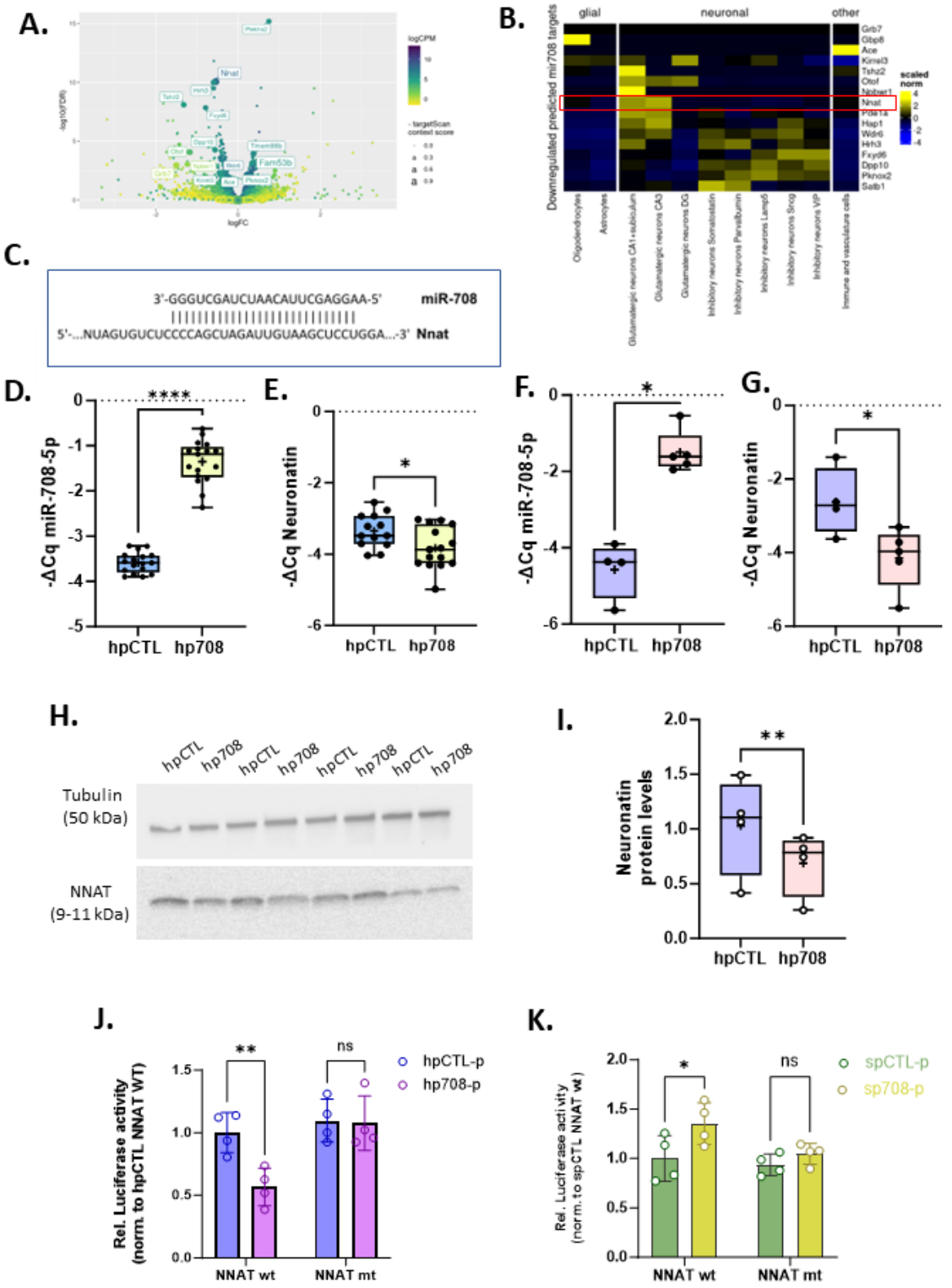
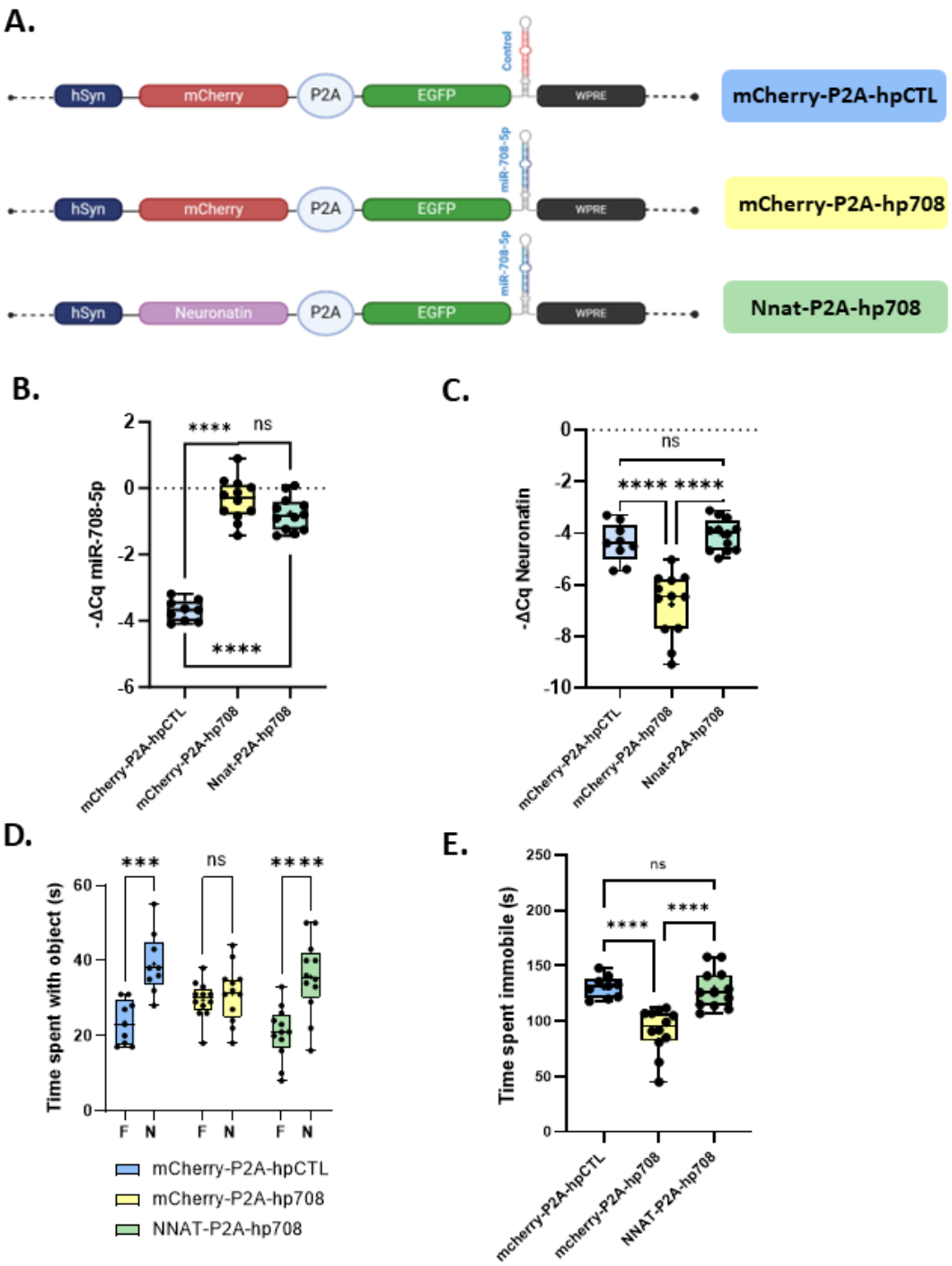
1282 **Figure 5. Restoring Nnat expression in miR-708-5p overexpressing**
1283 **hippocampal neurons rescues BD-associated behavior in mice.**